Nansen Environmental and Remote Sensing Center

NERSC Technical Report no. 275

Analysis of high-resolution satellite images for iceberg detection in the Barents Sea

Photograph of an iceberg drifting in sea ice. Courtesy: A. Glazovsky

Project for Hydro Oil and Energy 2006

Order no. 5356326 and 5383042

Authors:
Stein Sandven, Mohamed Babiker, and Kjell Kloster
December 2006

	Nansen Environmental and Remote Sensing Center (NERSC)
	Thormøhlensgate 47 N-5006 Bergen, Norway Phone: + 47 55 20 58 00 Fax: + 47 55 20 58 01 E-Mail: Stein.Sandven@nersc.no http://www.nersc.no

TITLE: **Analysis of high-resolution satellite images for iceberg detection in the Barents Seas**	REPORT IDENTIFICATION **NERSC Technical report no. 275**
CLIENT Hydro Oil and Energy	**CONTRACT** Order no. 5356326 and 5383042
CLIENT REFERENCE Lars Ingolf Eide	**AVAILABILITY** Customer report
INVESTIGATORS Stein Sandven, Mohamed Babiker, and Kjell Kloster	**AUTHORISATION** Bergen, 22 February 2007 Stein Sandven

Contents

Summary

In this project iceberg observations in the Northern and Eastern Barents Sea have been studied by use of high-resolution satellite images, supported by in situ observations from field expeditions by Arctic and Antarctic Research Institute in 2005 and 2006. Satellite images used in the studies include optical images from Landsat and Terra ASTER and Synthetic Aperture Radar (SAR) images from ENVISAT and RADARSAT. Images with resolution of about 15 m have been used, including alternating polarisation SAR images from ENVISAT. Since most of the icebergs in the Barents Sea are small, less than 100 m in horizontal extent, it was important to use relatively high resolution. Optical images give more reliable identification of icebergs of size 50 m and more compared to SAR, because SAR has high-frequency speckle noise disturbing the iceberg detection. On the other hand, optical images are limited by cloud and darkness, and the Barents Sea region is cloud cover most of the time. SAR can provide good data independent of cloud and light conditions, but iceberg observations are ambiguous and need to be confirmed by other observations. Iceberg detection depends also on the background conditions. Icebergs occur in (1) open water, (2) drifting sea ice, and (3) in fastice near coasts and in archipelagos. In fastice, studies showed that icebergs of 50 m or more could be well observed in optical and SAR images. In open water, SAR images can identify icebergs under moderate to low wind conditions, while optical images can be used in cloud-free conditions. The size of icebergs observable in open water was not studied in this project, but previous studies suggest that 100 m large icebergs are observable by the present satellites. Icebergs located in drifting ice are the most difficult to observe, because the background sea ice can have similar signature as the iceberg itself. The detection capability in all three situations can be improved by repeated use of satellite images. The project has reviewed data from previous Russian aircraft surveys to get an overview of the temporal and spatial distribution of icebergs. The interannual variability in iceberg distribution can be very large, and there is need for a monitoring system to control the extent and drift of icebergs. Scenarios for monitoring of icebergs are recommended where frequent coverage by satellite images is supplemented by aircraft and ship observations. Also tagging of selected icebergs by GPS/ARGOS transmitters will be an important part of a monitoring system. New high-resolution satellite images, both SAR and optical, will be available in near future. These data will improve the possibility to monitor icebergs from space.

1. Introduction

The icebergs in the Barents Sea originate from three main areas: Svalbard (in particular Nordaustlandet), Franz Josef Land and Novaya Zemlya. The most important area is Franz Josef Land with an estimated annual iceberg flux of 2.26 km^3. The flux from Novaya Zemlya and Svalbard is 2.00 km^3 and 1.65 km^3, respectively (Abramov, 1996). The probability of finding icebergs is also highest in Franz Josef Land area, with a mean annual probability occurrence above 80 %.

The size and shape distribution of the icebergs is such that the vast majority is of small scale, less than 20 m (bergy bits and growlers), while tabular icebergs, glacier bergs and other types at scales of 100 m or more represent a minority. This is a real challenge for implementation of monitoring systems. Aircraft surveys operated by Arctic and Antarctic Research Institute was the main monitoring method for several decades, but during the 1990s this survey has declined. In the last 15 years, there has been practically no iceberg monitoring by aircraft in the Barents Sea. Other observation methods include ship and polar station observations, but these have also declined in the last decade. Satellite observations have not been used regularly, but several research projects have demonstrated the possibilities to observe icebergs from satellite images.

The first studies of icebergs in the Barents Sea area using airborne SAR were conducted by Sandven et al., (1991) using images with about 10 m resolution. During the OKN IDAP programme 1988 – 1992, studies of iceberg calving and populations of drifting and grounded icebergs near the calving areas in Franz Josef Land were performed using high-resolution satellite images (Kloster and Spring, 1993).

The possibility to detect icebergs in the Northern Barents Sea by RADARSAR ScanSAR Narrow Far-Range images has been studied by Knapskog (1996). These images have a pixel size of 50 by 50 m, swath width of 300 km and incidence angle between 31° and 46°. His results show that detection capability is good for icebergs with horizontal scale of 200 m or more, drifting in open water under low wind conditions (< 10 ms^{-1}). Icebergs can also be detected at scales down to about 75 m, but with greater uncertainty. At scales above 250 m the shape of the icebergs can also be identified. The backscatter contrast between open water and identified icebergs was in the range 8 – 12 dB at incidence angle around 40°. When the wind speed increases above 10 ms^{-1} or when sea ice is present, the backscatter contract between icebergs and the surrounding surface is rapidly reduced. The detection capability is thereby greatly diminished.

Iceberg observations in high resolution optical images is not hampered by the speckle noise which is characteristic for the SAR images. Observations in optical images are therefore more reliable for icebergs of size of 100 m or less. The limitation of optical images is cloud cover and darkness, allowing good quality observations only occasionally. Since the first studies of icebergs using Landsat, SPOT and airborne SAR data two decades ago, there are now more satellite systems producing high-resolution images which can potentially improve the capability of monitoring icebergs. In this study, we have tested use of alternating polarization SAR images from ENVISAT, RADARSAT ScanSAR Narrow images, optical images from Landsat and ASTER, and the possibility to monitor icebergs in the Barents Sea with optical and SAR images over a period of four months. The results of this study are presented in this report with recommendations for further development of an iceberg monitoring system for the Barents Sea region.

2. Satellite data used in the study

The availability of high resolution satellite images from archives for the IDAP period was investigated, because extensive observations of iceberg occurrence and iceberg properties were obtained in this period. However, only limited amount of satellite images are available for the

period 1988 – 1992. SAR data from satellites started in August 1991, but very few images covered the iceberg areas in the Barents Sea. Also the satellite data from archives from 1992 to present have been searched for high resolution images, but the number of images covering the most important iceberg areas was limited.

The present study has therefore focused on acquisition and analysis of satellite data from 2005 and 2006, where also in situ and aircraft observations from field expeditions from AARI have been provided. In the last 2 – 3 years the amount of high resolution satellite images covering the iceberg areas has increased significantly. This is mainly due to the production of Terra ASTER images and the production of SAR data from RADARSAT as well as from ENVISAT. An example of data coverage by Terra ASTER in Franz Josef Land is shown in Fig. 1, where quicklook images with little or no clouds have been retrieved from the ASTER image archives. The Landsat ETM+ and Terra ASTER images used in the study were provided by the USGS EROS data center. The ENVISAT ASAR data were provided by European Space Agency and the RADARSAT image was provided by Kongsberg Satellite Services, the distributor of RADARSAT data in Norway. The technical specifications of the images used in the study are listed in Table 1.

Table 1: Satellite image specification

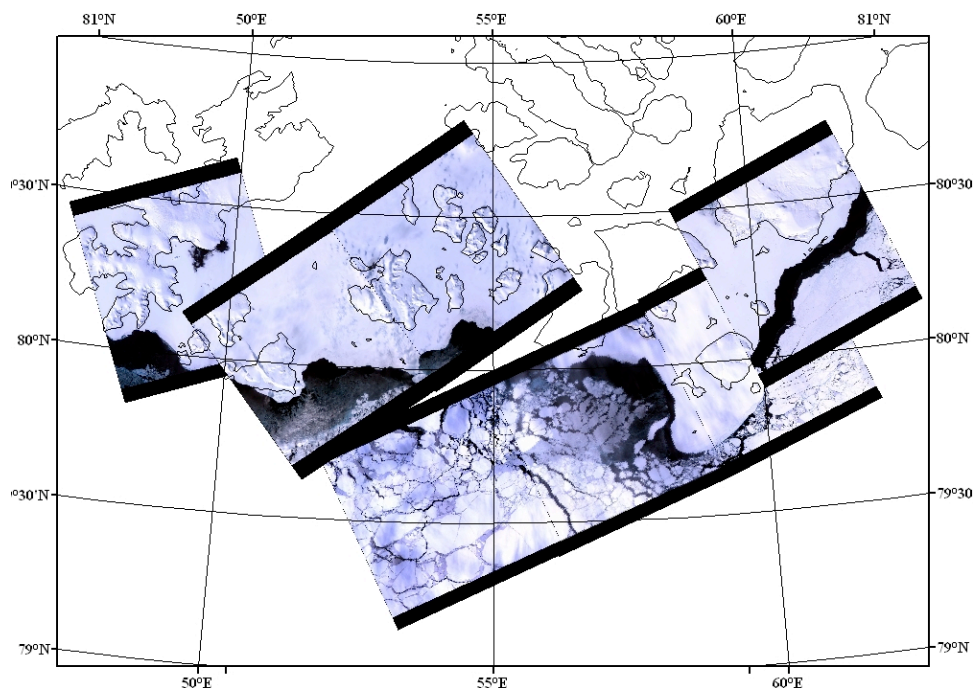| Satellite sensor	Image mode	Pixel size	Image size/Swath width
Landsat ETM+	Panchromatic	12.5 m	180 by 180 km
	Multichannel	25 m	180 by 180 km
Terra ASTER	Panchr & multichannel	15 m	60 by 60 km
ENVISAT ASAR	Wideswath	75 m	400 km
	Alternating polarisation (HH- and VV polarisation)	12.5 m	100 km
RADARSAT	ScanSAR Narrow mode	25 m	300 km

Figure 1. Mosaic of ASTER quicklook images with little or no cloud cover in the Franz Josef Land area in spring 2005. The images cover a large part of the iceberg producing areas in the archipelago. Each image covers 60 by 60 km. Images were provided by the USGS EROS data center.

3. Image analysis for 2005

Satellite images from ASTER were mainly selected for the month of April when in situ observations from the AARI expedition were obtained. A table of iceberg positions from the report by Danilov et al., (2005) was used to plot the location of icebergs as shown in Fig. 2, where also the quicklooks of the ASTER images are shown. A total of 10 ASTER images were selected for further analysis based on co-location with in situ data. The area north of 75N was generally covered by sea ice in this period, as shown in the ice charts (Fig. 3). Along the coast of Novaya Zemlya the ASTER quicklook images show a polynya with thin ice, indicated by dark signature in the optical images. SAR data were not used in the 2005 study, but AARI had analyzed a few RADARSAT ScanSAR narrow scenes in the area south of Franz Josef Land. The location of the icebergs retrieved for the RADARSAT images are included in the list provided by AARI. The iceberg position from the RADARSAT data are plotted by green triangles in Fig. 3, and they are compared by ASTER observations described in the next section. The detection of icebergs was performed for three different ice conditions: in fast ice near land and islands, in open water or thin ice in the polynyas, and in the drifting pack ice where ice concentration and floe size varied significantly.
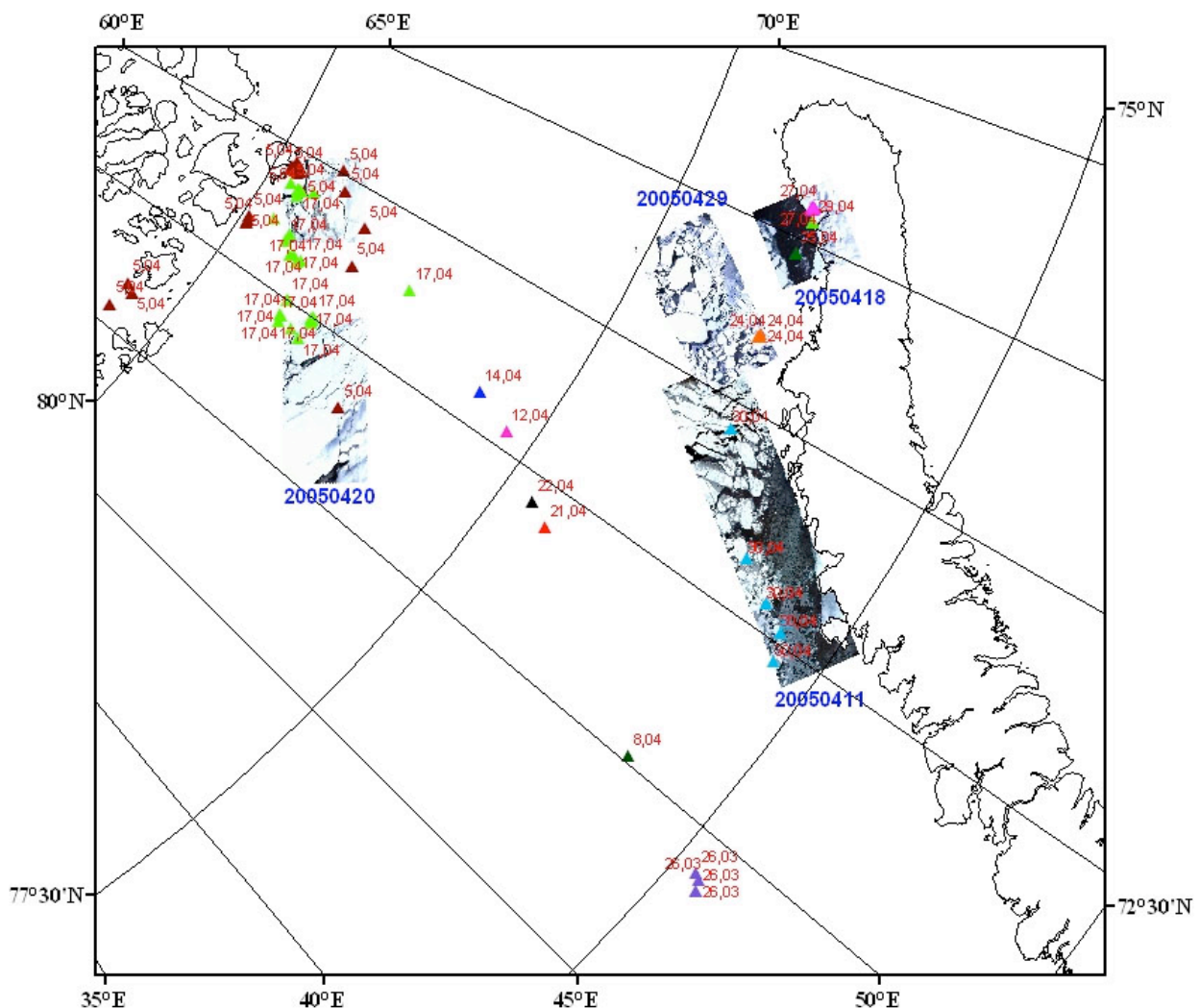

Figure 2. Map of the study area in 2005 showing the location of the ASTER images obtained in April and in situ observations from the AARI expedition marked by triangles and date of observation. The date of each ASTER image stripe is also indicated: 11, 18, 20 and 29 April.
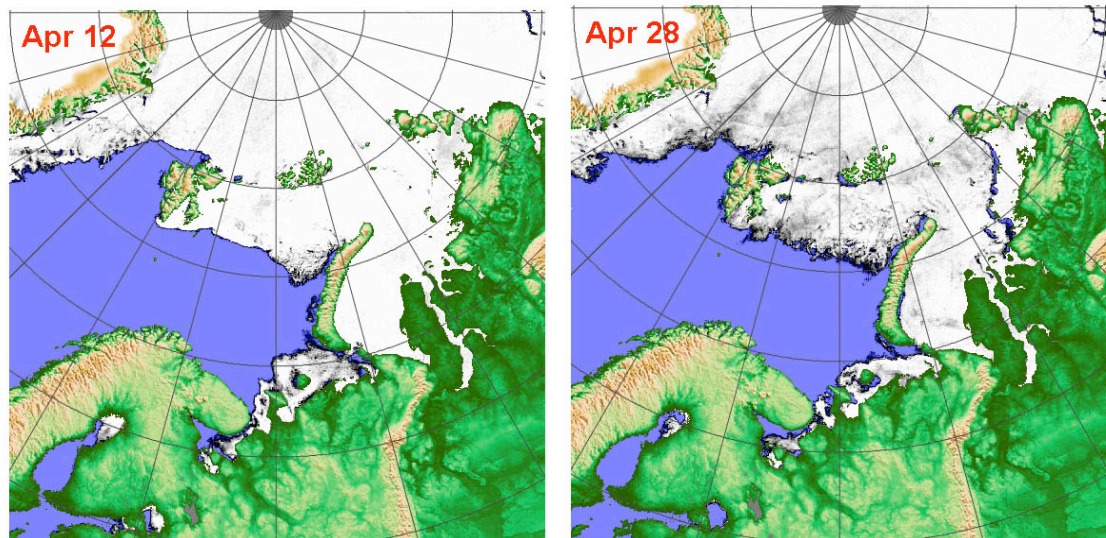
Figure 3. Ice charts from AMSR-E data for 12 and 28 April 2005, showing the general sea ice extent in the period of the iceberg analysis. Courtesy University of Bremen.

3.1 South of Franz Josef Land

The analysis of the optical images for detection of icebergs is based on identification of bright objects with a characteristic dark shadow caused by the sun angle. This criterion is quite reliable for icebergs embedded in fastice. Example of this detection is shown in Fig. 4a. In the three images from 20 April obtained south of Franz Josef Land, a total of 245 icebergs were found in an area of about 10.000km^2 (Fig. 4b). The size of the detected icebergs was typical 50 m or more. The possibility to detect icebergs under different background conditions is discussed in subsequent examples and in the conclusion chapter.
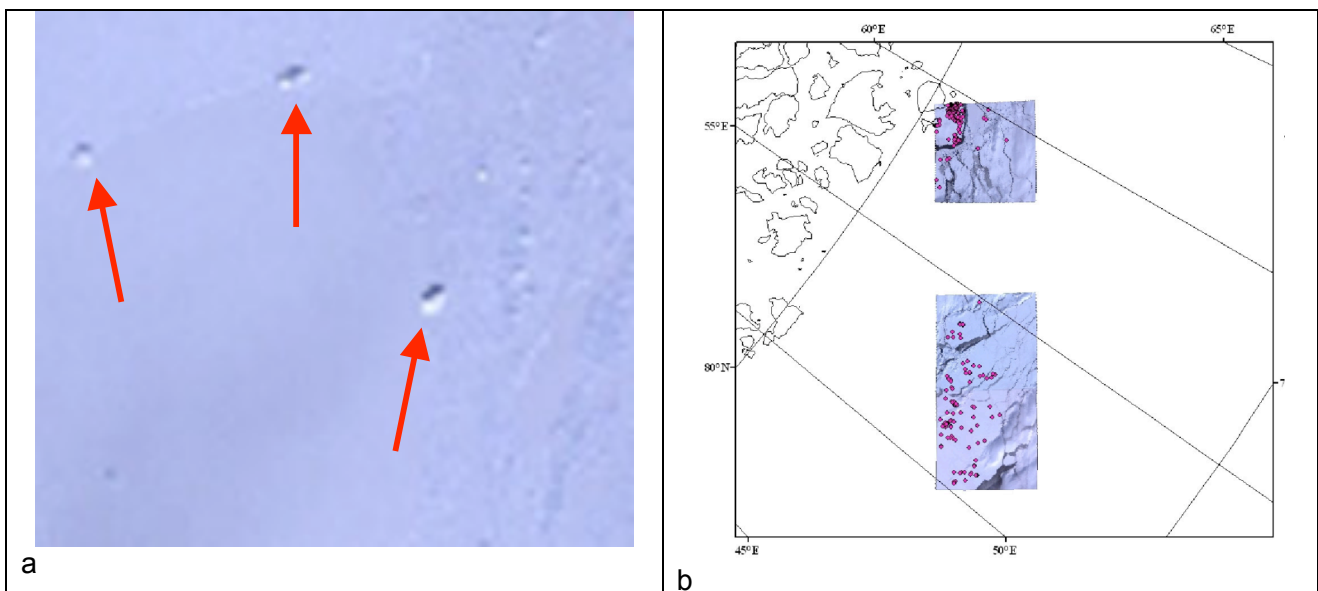

Figure 4. (a) Detection of icebergs located in fastice using optical images. The characteristic bright spots and dark shadows suggest that features are icebergs. (b) Three ASTER images from the 20 April 2005 which have been analyzed for icebergs. The location of the 245 detected icebergs are superimposed as red dots.

The upper image of Fig. 4b (located to the northeast) is zoomed in and presented in Fig. 5, showing the highest number of icebergs in the fastice to the south of Salm Island, one of the iceberg producing areas of Franz Josef Land. Detection of icebergs in optical images is most feasible in level fastice where the background is fairly homogeneous, as shown in Fig. 4a. Icebergs can also be detected in drifting ice in the case of large floes with similar characteristics as the fastice. For small floes and various stages of deformed sea ice drifting in the Barents Sea, it is more difficult to detect icebergs mainly because of more „noisy" background. Detection of icebergs using RADARSAT Standard Images was performed by AARI in the same area as the ASTER images. The analysis of the RADARSAT images, obtained on 05 April, showed a number of icebergs with locations reported by Danilov et al., (2005). These locations are plotted on top of the ASTER image (Fig. 5) and marked by the date: 05.04. There are many more icebergs observed in the optical image compared to the SAR image. This needs to be verified, but we did not have access the SAR image so we could not perform digital analysis and comparison of the two types of images.
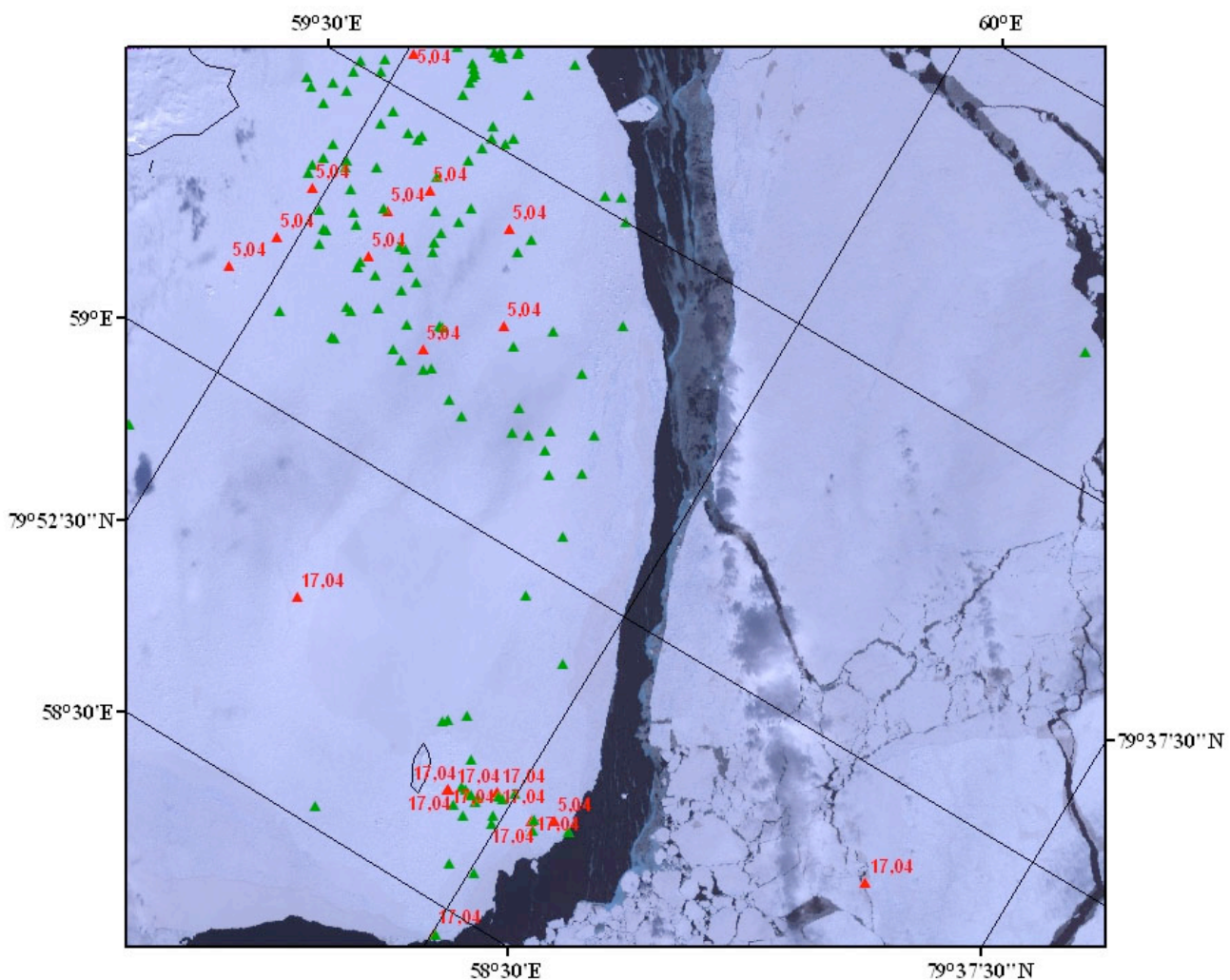
Icebergs spatial distribution (red from the report and the date is indicated) green from the aster image dated 20050420

Figure 5. Zoom-in on one of the ASTER images from the 20 April 2005 with location of icebergs from image analysis superimposed by green triangles and observed icebergs from the AARI expedition (red triangles marked 17.04). The red triangles marked 05.04 are obtained from RADARSAT SAR image analysis reported by AARI (Danilov et al., 2005).

Comparison between ASTER observations and in situ observations from helicopter flights are shown in Fig. 6, which is a further zoom-in of the lower part of Fig. 5. In addition to the identified icebergs from the image analysis, marked by the red dots, there are also areas with smaller objects can be interpreted as small icebergs or other topographical features such as ridges. Many such features are found inside the red and yellow polygons in Fig. 6, but they are not included as icebergs in our analysis. The total number of 245 icebergs identified in the three ASTER images is therefore a conservative estimate. If we had used images with higher resolution, for example SPOT images with 5 m pixels, the number of detected icebergs would have been higher. Note that there is only three days between the helicopter observations and the ASTER image, and that the helicopter observations are very near the icebergs identified in the ASTER image. Thus, the helicopter observations confirm that the iceberg retrieval from the image analysis is correct.
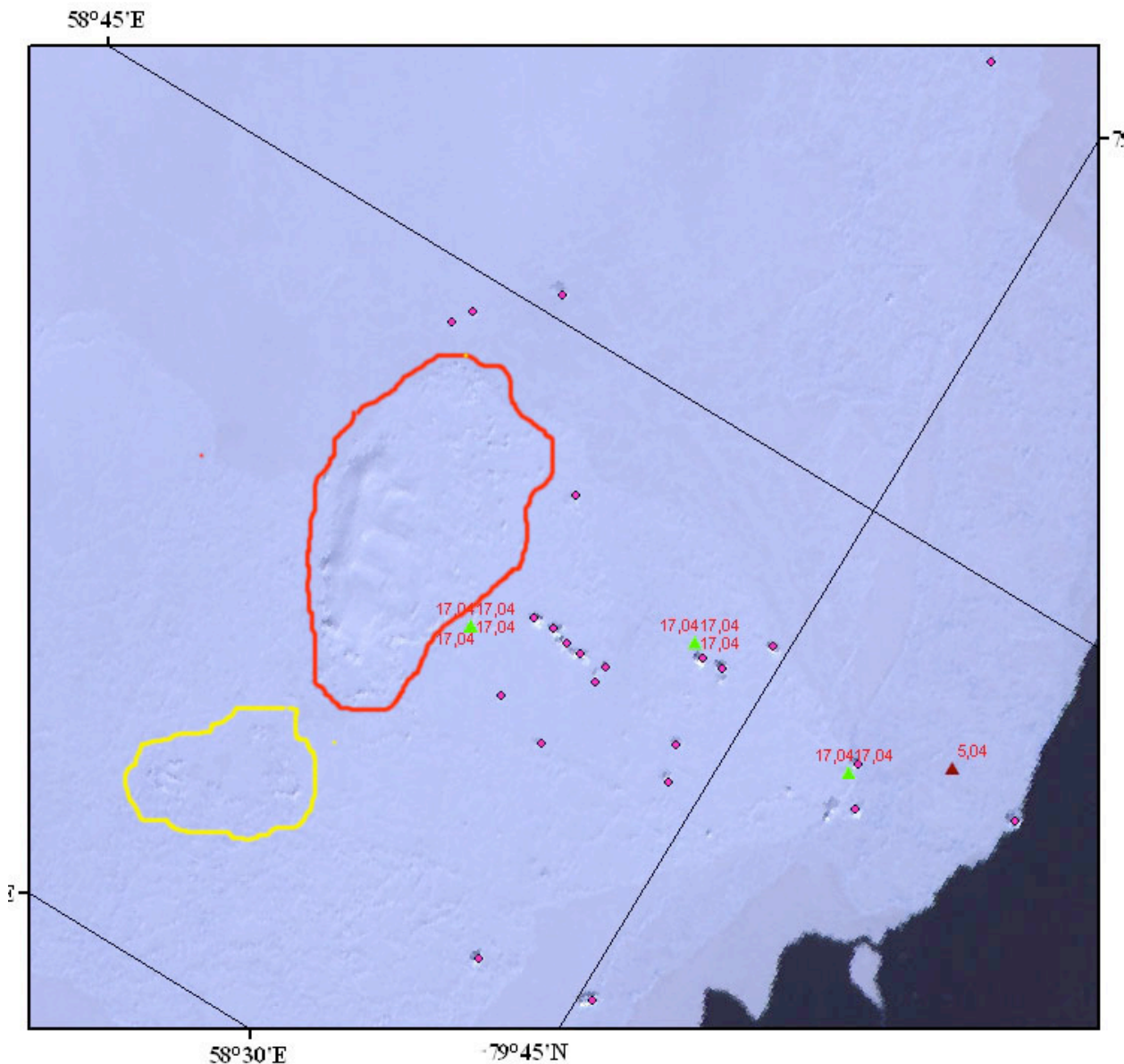

Figure 6. Zoom-in of the ASTER images in Fig 5 (from the 20 April 2005) with location of icebergs from image analysis (red dots) superimposed by green triangles which are observed icebergs from helicopter flights on 17.04. The red and yellow polygons mark areas where more icebergs are likely to be found.

3.2 Time sequence of images south of Franz Josef Land

The area south of Salm Island was covered by ASTER images on 20 April, 09 May and 18 June, allowing us to look at repeated images over roughly the same area, as illustrated in Fig. 7. The three images show that the fastice area around the islands did not change much in the period and that most of the icebergs were located in the fastice area. Icebergs embedded in the fastice are stationary as long as the fastice is not moving. Detection of these icebergs is more feasible because the background is generally homogeneous and time of observation is less critical. It is noteworthy that many icebergs can also be detected in open water between the fastice and the drifting ice, especially on 18 June. A few icebergs are also observed in the drifting ice in the 20 April image.
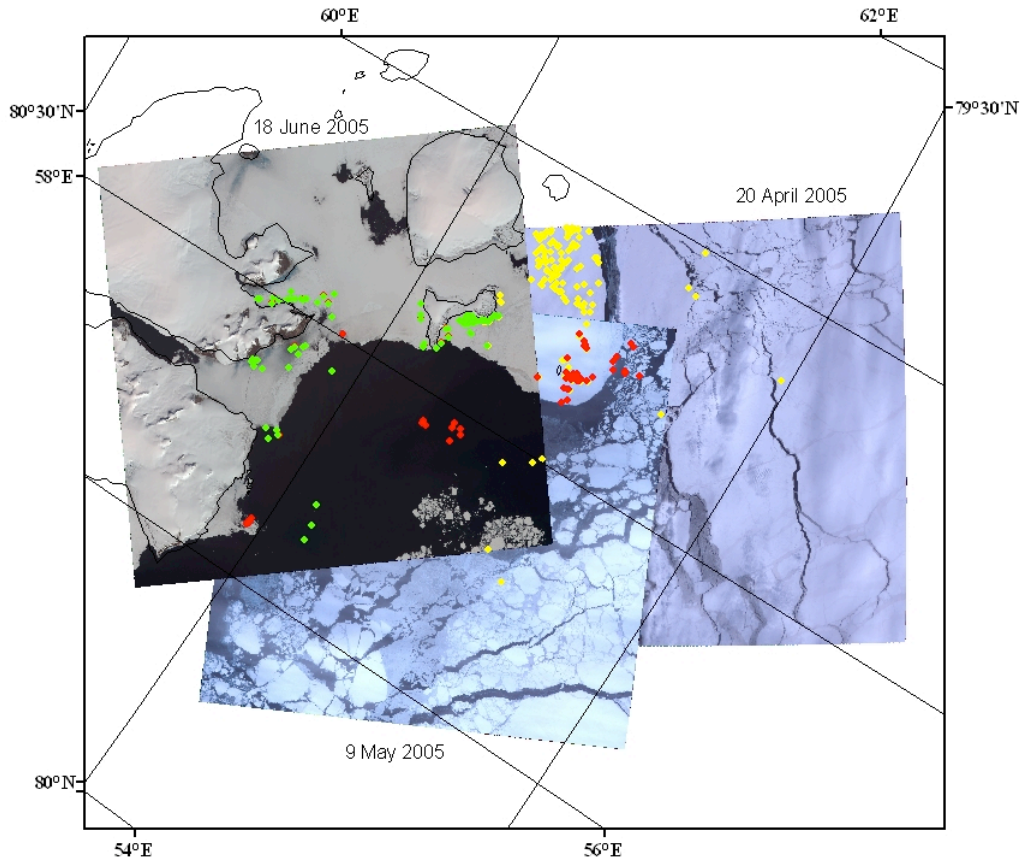

Figure 7. Composite of three ASTER images centred at 80 N and 58 E, in the southern part of Franz Josef Land. The dots indicate location of icebergs from image analysis on 20 April (yellow dots), 09 May (red dots) and 18 June (green dots).

The changes in iceberg numbers and locations have been checked for the fastice area where there is overlap between all three images. The results shows that the same icebergs are found in all three images, suggesting that the icebergs near the coast have not started to move away by 18 June. Even if the fastice boundary have changed from 09 May to 18 June, the iceberg locations are unchanged, as shown in Fig. 8. The red dots are icebergs from the 09 May image, while the green dots are from the 18 June image. The red and green dots are exactly on top of each other, showing that the icebergs have not moved. This is also the case for the two icebergs which are inside the fastice on 09 May and outside the fastice on 18 June. Another large iceberg, located in

the lower part of the images (Fig. 8) has moved very little even if the surrounding sea ice has moved. This suggests that several of the icebergs are grounded. The total number of icebergs identified in the images are 245 on the 20 April images (3 images), 138 on the 09 May image and 86 on the 18 June image. Many of the same icebergs have been observed two or three times.
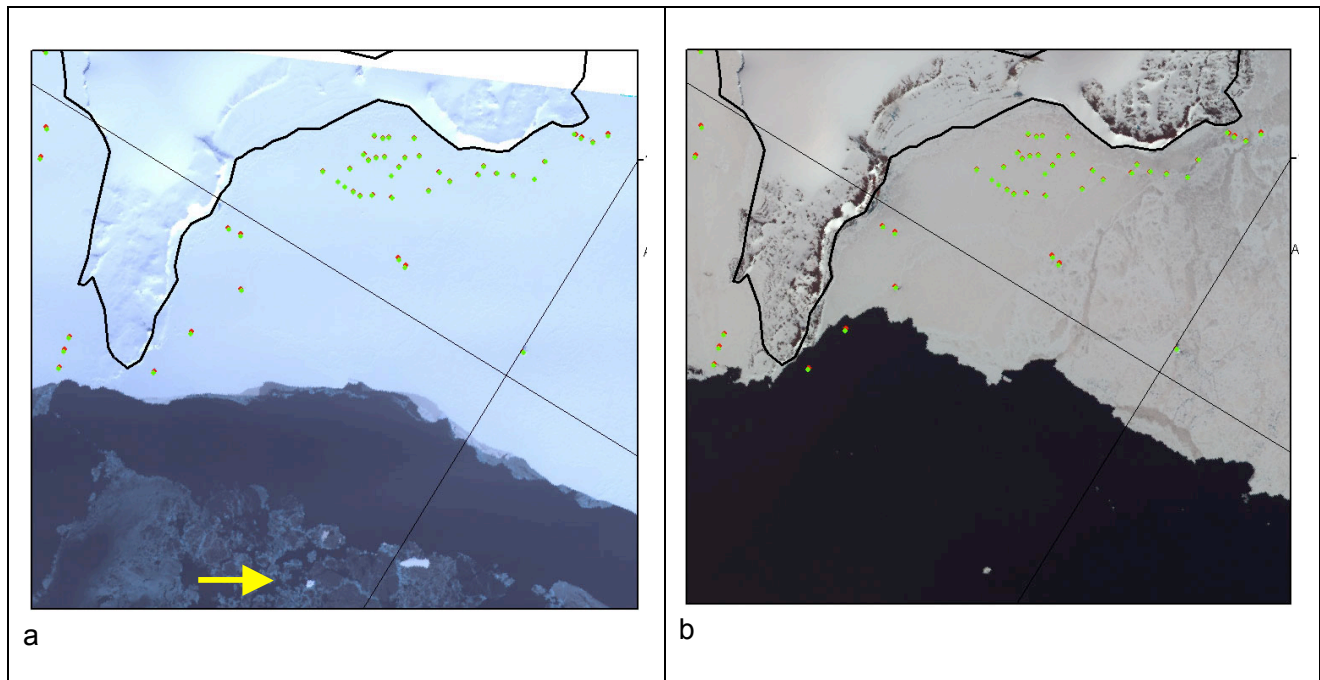

Figure 8. Subsets of the ASTER images obtained on 09 May 2005 (a) and 18 June 2005 (b) with location of identified icebergs. Red dots: icebergs from 09 May, green dots: icebergs from 18 June. The arrow indicate a large iceberg which stays approximately in the same area outside the fast ice area during the period, suggesting that the iceberg is grounded.

3.3 Icebergs along the coast of Novaya Zemlya

During April, ASTER images were obtained off the west coast of Novaya Zemlya on the 11th (4 images), the 18th (1 image) and on the 29th (2 images), as shown in Figure 9. All three images have in situ validation data indicated by triangles and date of observation. The images have been analyzed for icebergs and identified icebergs are shown by dots superimposed in the images. The 11 April image (Fig. 10) shows that most of the icebergs are located in the fast ice near the coast, one is found in the thin ice of the coastal polynya, and four icebergs are found in the drifting firstyear ice. Since there is a time difference of 19 days (from 11 to 30 April) between satellite and in situ observations, we cannot expect to find the icebergs in the same position in the two data sets. We can only assume that some of the four icebergs in the satellite image may be among the five observed during the field observations 19 days later. The image from 18 April (Fig. 11) is obtained about ten days before the in situ observations, but unfortunately the icebergs observed in the fast ice during the expedition could not be found in the images because of cloud cover. The icebergs for the image analysis are located in areas not covered by the in situ observations. This was the case also for the last image (Fig. 12), which was obtained five days after the in situ observations. It is expected that the iceberg documented by in situ observations on 24 April drifted out of the image obtained on 29 April. Hence, direct validation of the satellite observations could not be done in this case. The image analysis, however, showed that more than 20 icebergs were found in different parts of the 60 by 120 km large area covered by drifting ice.
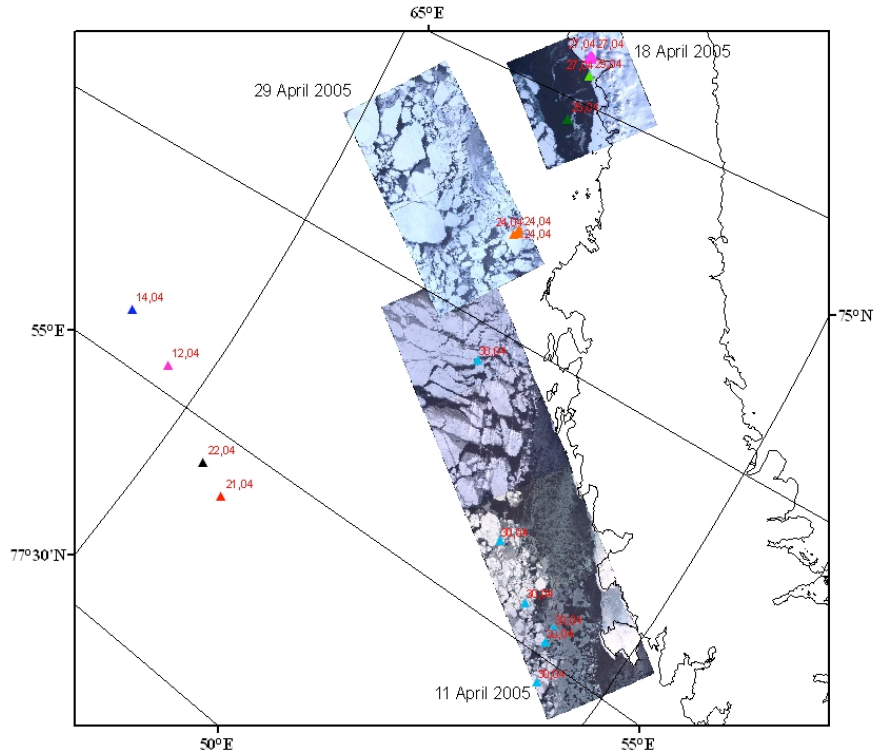
Figure 9. Overview of ASTER images and position of in situ iceberg observations off the coast of Novaya Zemlya. Each iceberg is marked by a triangle with date of observation.
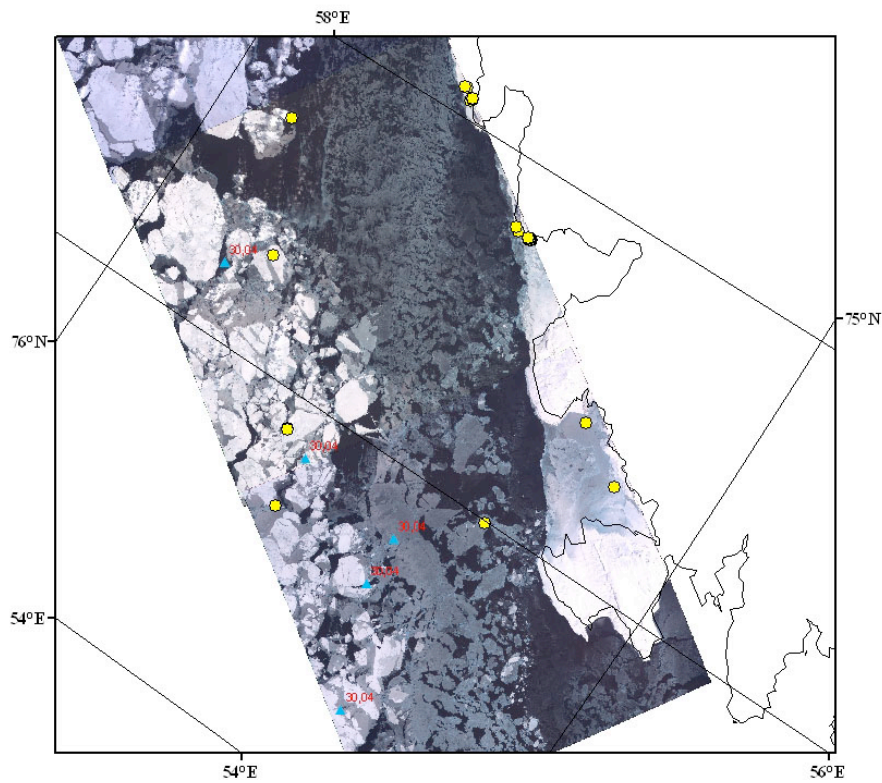

Figure 10. Iceberg locations from ASTER image analysis from 11 April (yellow points) and position of in situ iceberg observations (triangles with date of observation) off the coast of Novaya Zemlya.

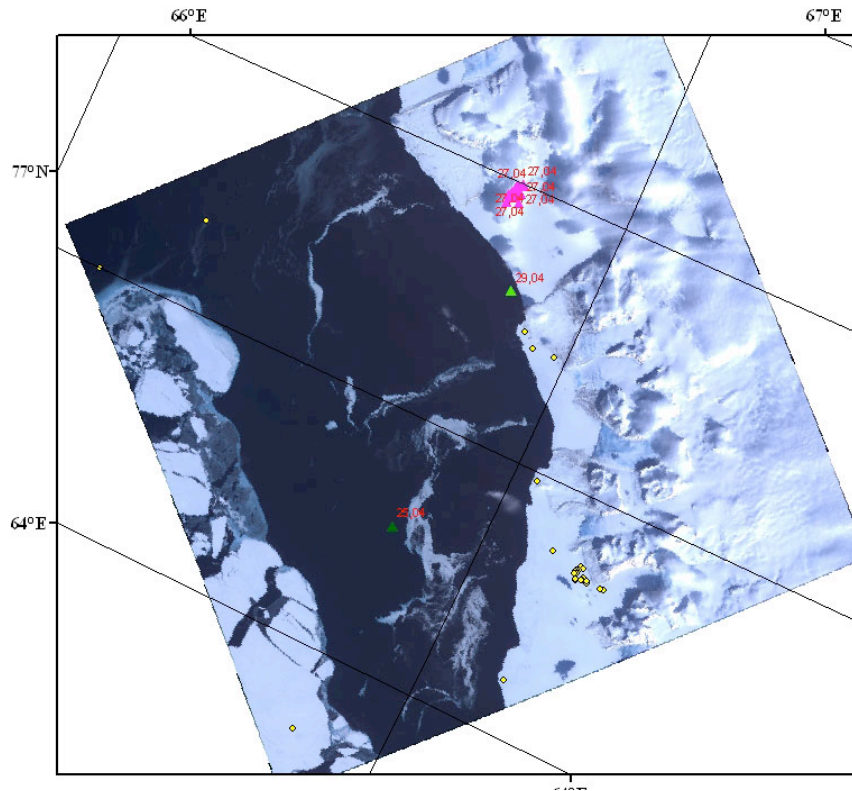*Figure 11. Iceberg locations from ASTER image analysis from 18 April (yellow dots) and position of in situ iceberg observations (triangles with date of observation) off the coast of Novaya Zemlya.*
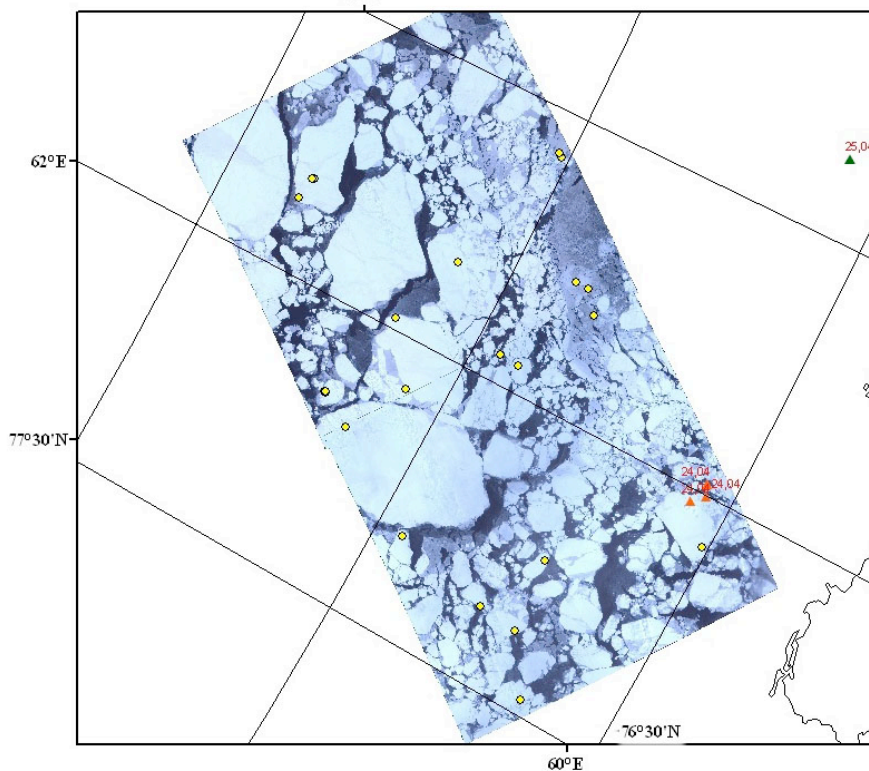

Figure 12. Iceberg locations from ASTER image analysis from 29 April (yellow dots) and position of in situ iceberg observations (triangles with date of observation) off the coast of Novaya Zemlya.

4. Image analysis for 2006

While the satellite data for 2005 had been collected from archives without any pre-ordering, the work for 2006 was planned in advance allowing ordering of satellite data for specific regions and time periods. This made it possible to have both ASTER and Landsat images as well as some SAR images from RADARSAT and ENVISAT. From ENVISAT we ordered alternating polarisation images that matched some of the optical images, allowing direct comparison of icebergs observation from different types of satellite data. The satellite data acquisition was also planned to be simultaneous with field observations by ship and aircraft. This was only partly successful because satellite data need to be ordered at least two weeks in advance while ship and aircraft tracks are often changed according to weather and ice conditions. The data collection started in March – April, supporting the Somov expedition organised by AARI. It continued through the summer to supplement an aircraft survey in July and to investigate the distribution of icebergs through the summer months.

4.1 Satellite and field observations in March-April

In March-April several Landsat, ASTER and SAR images from RADARSAT and ENVISAT were obtained in the coastal regions of Franz Josef Land and Novaya Zemlya. The image ordering and acquisition was coordinated with planned ship tracks and iceberg observations from the Somov expedition. The in situ observations of icebergs from the Somov expedition are plotted in Fig. 13a where also three Landsat and one ASTER image are shown. The general ice conditions was characterized by open waters extending far north and large coastal polynyas to the northwest of Novaya Zemlya as well as Franz Josef Land (Fig. 13b). The coastal lead is identified by dark signature in the optical image on the northwest coast of Novaya Zemlya.

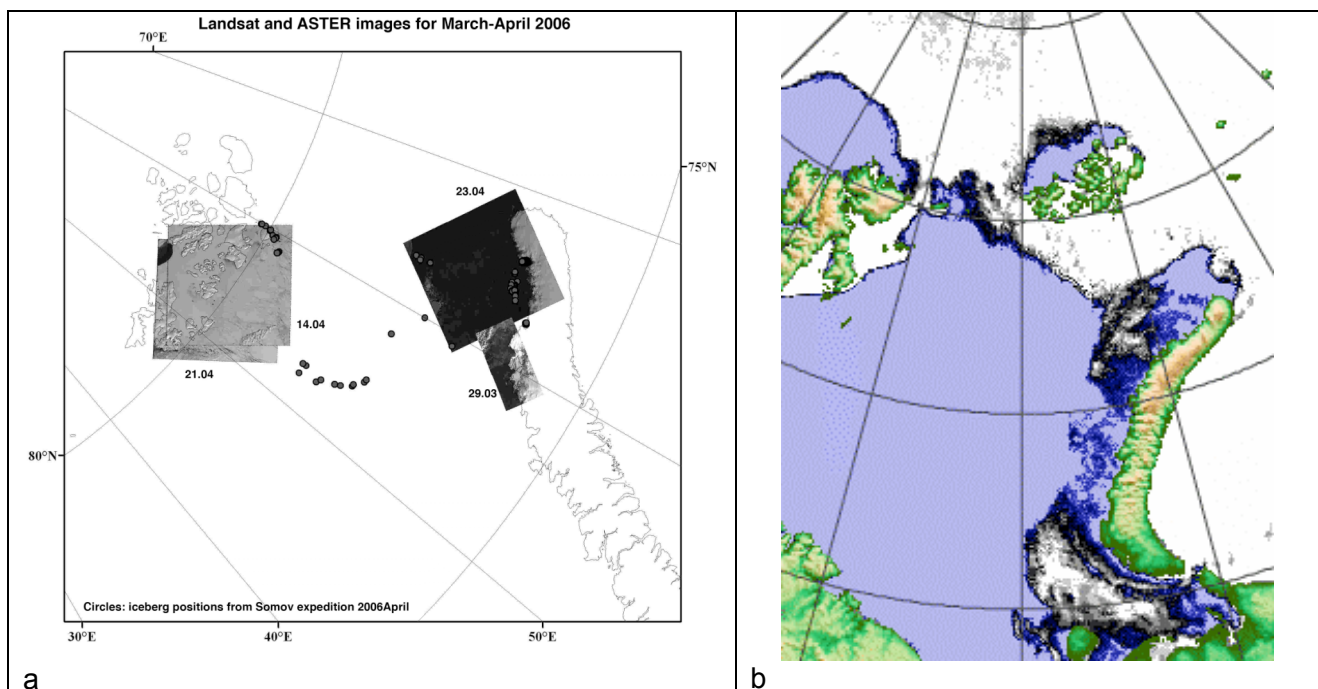*Figure 13. (a) Three Landsat images (180 by 180 km) and one ASTER image stripe (60 by 120 km) shown in combination with in situ iceberg observations (dots) from the Somov expedition; (b) sea ice extent and concentration map for 24 April, 2006, produced from passive microwave satellite data (Courtesy: Institute of Environmental Physics, University of Bremen). The greyish to dark signature means ice concentration below 50 %.*
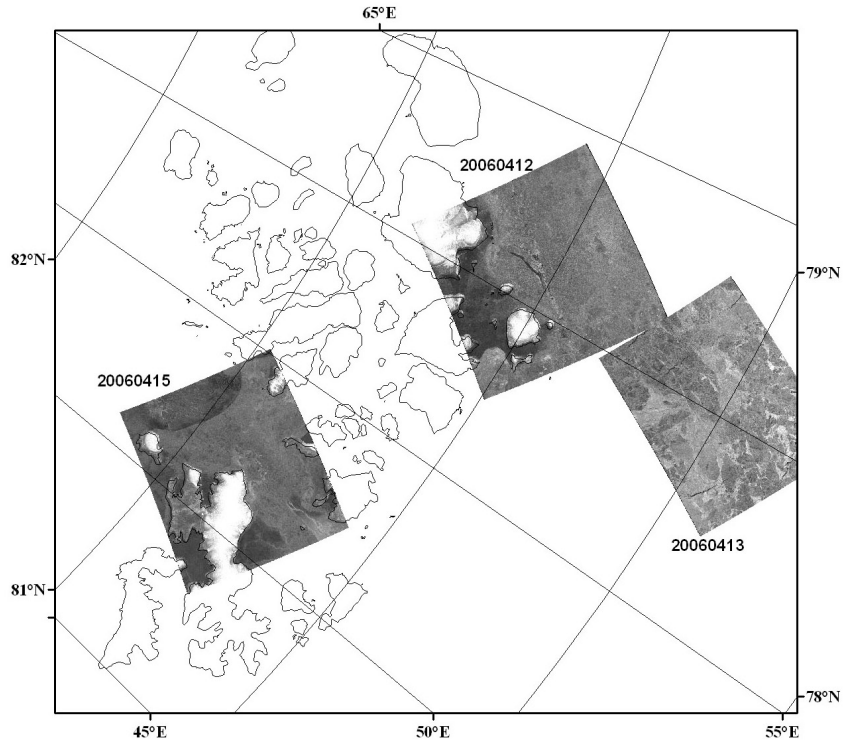
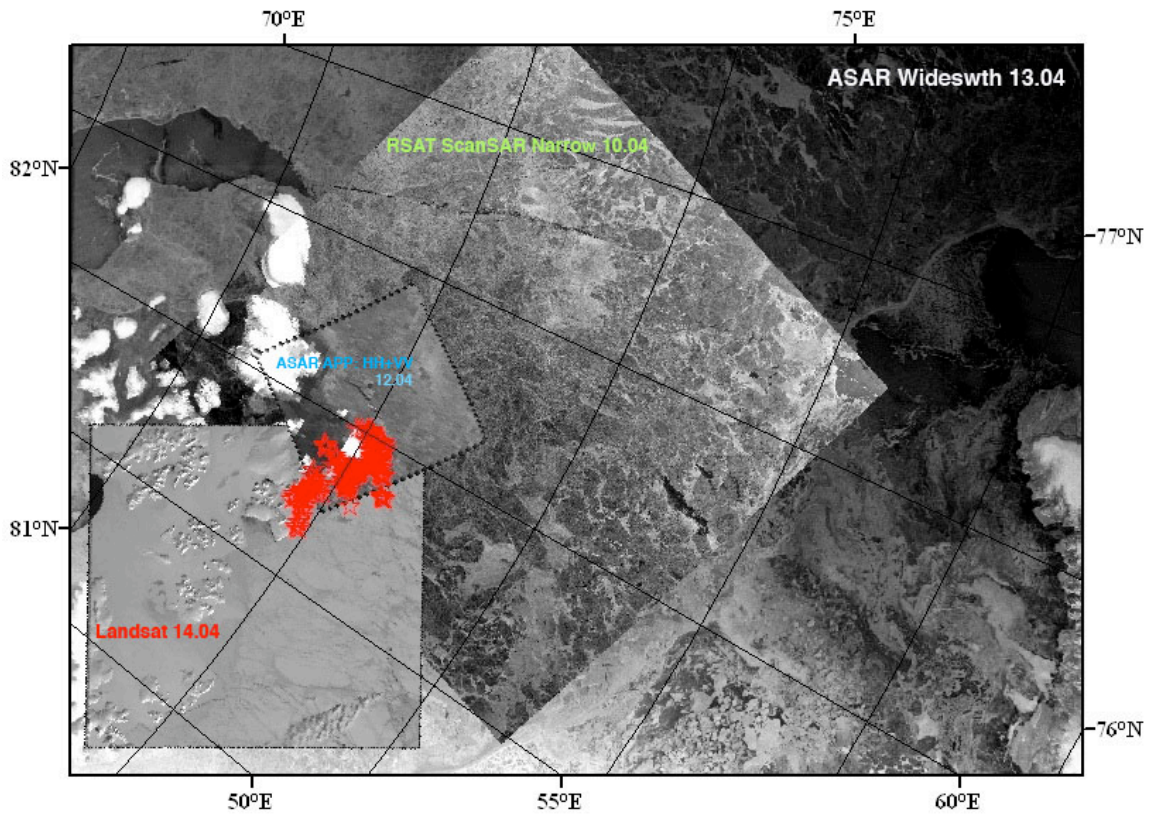*Figure 14. Location of three ENVISAT ASAR Alternating Polarisation images from April 2006.*

Figure 15. Co-located images from ASAR Wideswath (13.04), RADARSAT ScanSAR Narrow (10.04), ASAR HH- and VV-polarisation (12.04) and Landsat (14.04). The red markers show location of icebergs in the overlapping area between the Landsat and the SAR images.

The first Landsat image in Franz Josef Land was obtained on 30 March (Fig. 16a), showing a large coastal polynya on the southern side of the archipelago. The passive microwave ice chart shows clearly the polynya south of Franz Josef Land (Fig. 16b). This area was repeatedly covered by new Landsat images on 14 and 21 April.
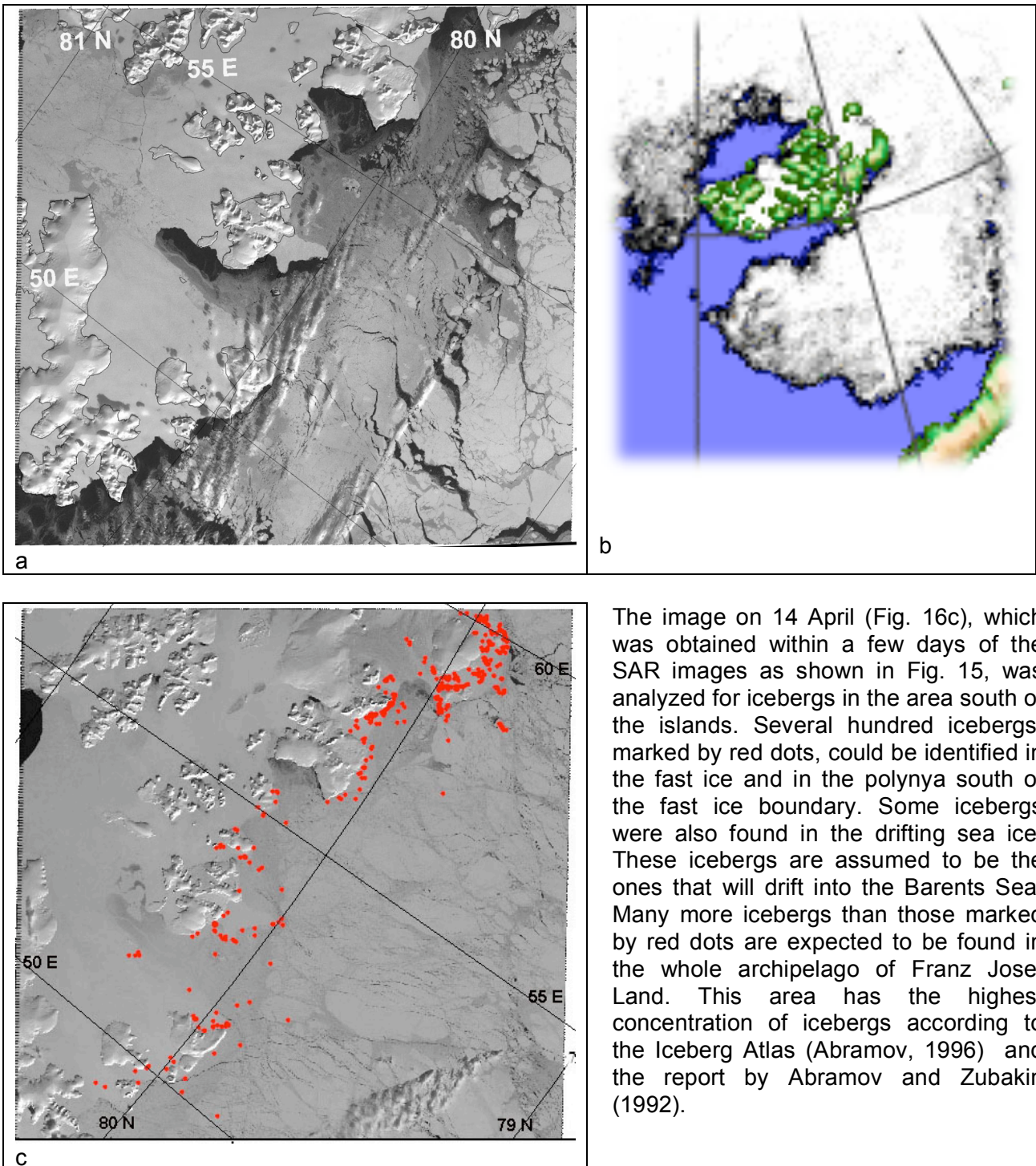
The image on 14 April (Fig. 16c), which was obtained within a few days of the SAR images as shown in Fig. 15, was analyzed for icebergs in the area south of the islands. Several hundred icebergs, marked by red dots, could be identified in the fast ice and in the polynya south of the fast ice boundary. Some icebergs were also found in the drifting sea ice. These icebergs are assumed to be the ones that will drift into the Barents Sea. Many more icebergs than those marked by red dots are expected to be found in the whole archipelago of Franz Josef Land. This area has the highest concentration of icebergs according to the Iceberg Atlas (Abramov, 1996) and the report by Abramov and Zubakin (1992).

Figure 16. (a) Landsat image from the southern Franz Josef land area obtained on 30 March, showing a large polynya to the south of the fast ice in the archipelago; (b) ice chart from 27 March based on passive microwave data produced by Institute of Environmental Physics, University of Bremen; (c) Landsat image from 14 April with identified icebergs marked by red dots.

Two images covering the north-western coast of Novaya Zemlya (Fig. 17 and 18) were analyzed for icebergs, showing that icebergs can be found along the whole coastal region.
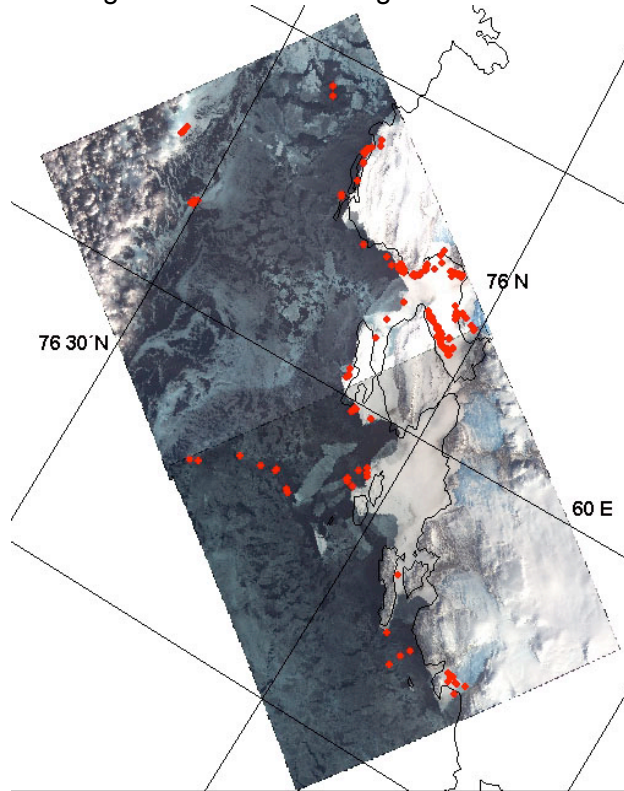
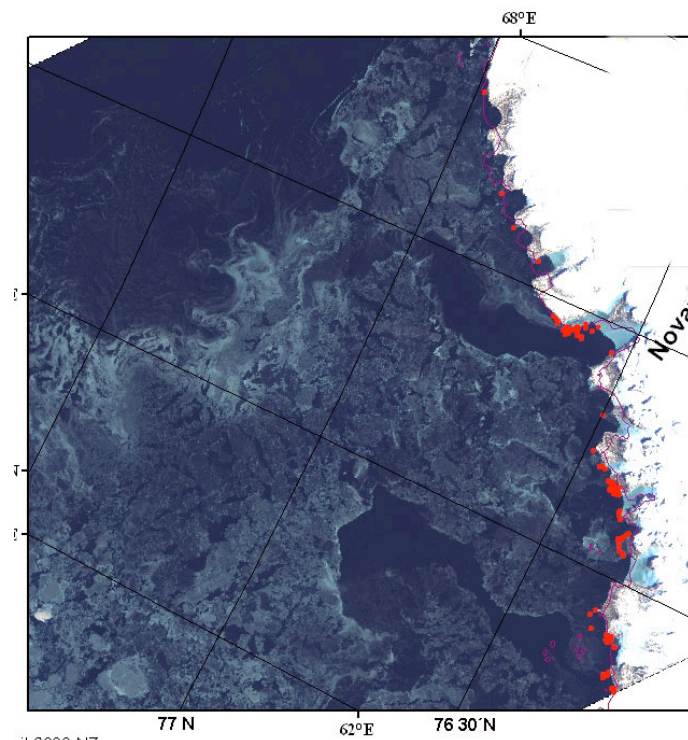*Figure 17: ASTER image of 29 March 2006 with iceberg analysis (red dots)*

Figure 18. Landsat image of 23 April 2006 with iceberg analysis (red dots).

4.2 Satellite and field observations in June-July-August

Ordering, acquisition and analysis of satellite images continued during the summer months of 2006, focusing on optical images in the area from Franz Josef land to northern part of Novaya Zemlya (Fig. 19). The purpose of the summer data was to (1) support operations in the Shtokman area and to complement an aircraft survey for iceberg detection on 27 July (Fig. 20), and (2) study the iceberg distribution in the summer months compared to the situation in April. Landsat image acquisition was therefore ordered continuously in the northern and eastern parts of the Barents Sea for the whole summer period. Good quality Landsat images and ASTER images available from archives were ordered and analyzed. The images presented in the overview maps (Fig. 19 and 20) include all the available images of good quality, i.e. with minimum cloud cover.
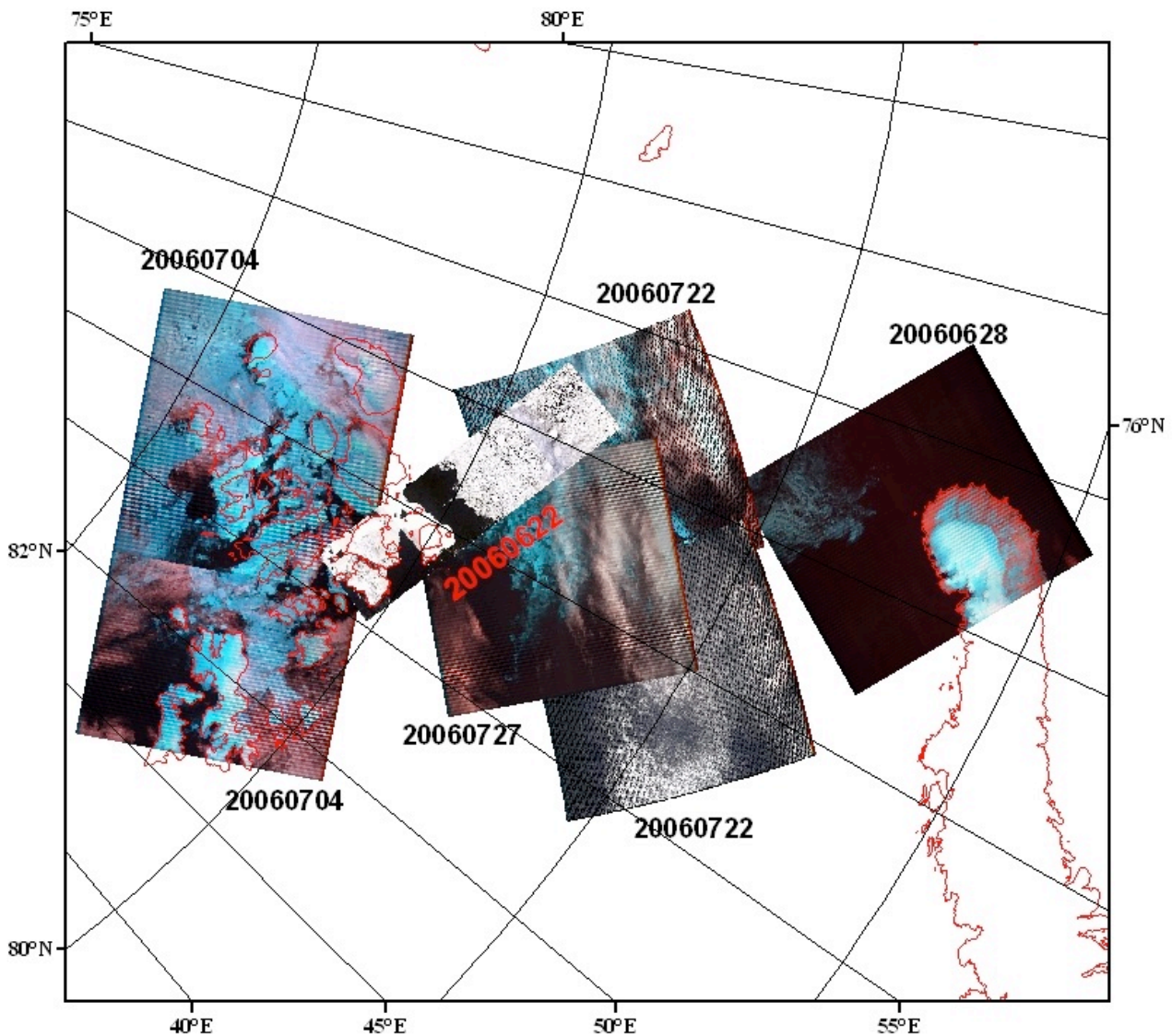

Figure 19. Composite map of six Landsat and four ASTER quicklook images, combined into one strip, obtained in the northern Barents Sea during June and July 2006. The dates for each image are indicated. All images except for the northernmost Landsat images (from 04 July) were analyzed for iceberg detection.

An iceberg surveillance flight was conducted by AARI on 27 July, as shown in Fig. 20, to find possible icebergs in the Shtokman area and further north. Landsat data were continuously ordered during July and August, but the only images obtained in the area of the aircraft survey were obtained one month later, on 26 August. These images did not show any signs of icebergs. However, the images obtained further north, between Franz Josef Land and northern part of Novaya Zemlya, showed many icebergs. The northern coast of Novaya Zemlya showed one iceberg located in open water at 76.86 N 64.37 E with a size of about 380 m (Fig. 21). Iceberg detection in open water is straightforward using optical images, where the background is dark and icebergs have bright signature. With the presence of sea ice, it is difficult to identify any icebergs. As seen in the upper left part of the Fig. 21, the signature of the sea ice is bright, bluish, when three channels in the Landsat image are combined.
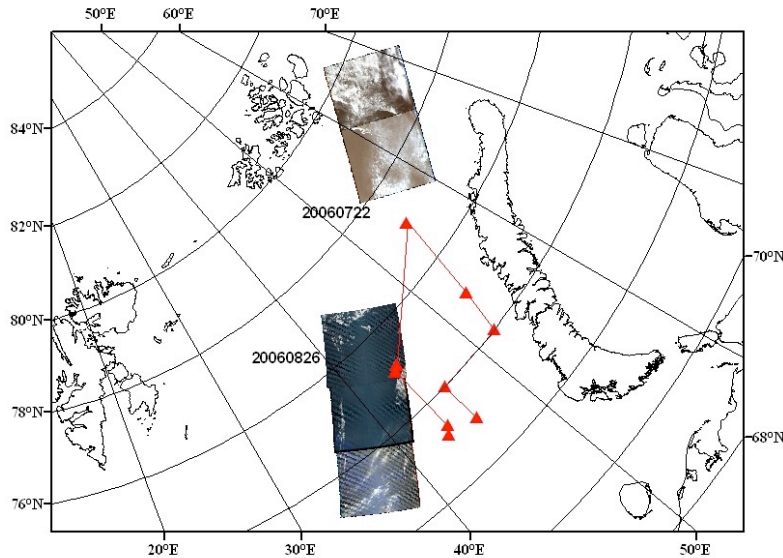
Figure 20. Landsat images with minimum cloud cover obtained before and after the aircraft surveillance flight on 27 July, indicated by red triangles and lines, conducted by AARI.
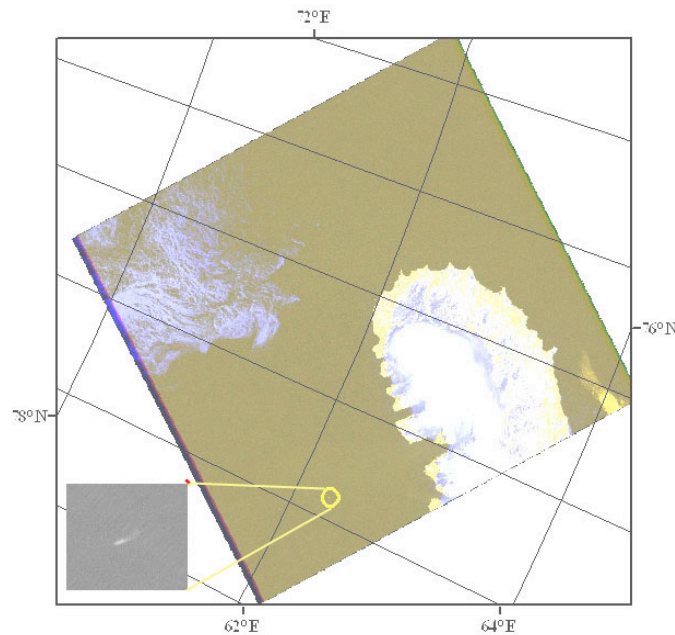
Figure 21. Landsat image (28 June) showing iceberg as a bright object against dark background.

Another example of channel combination in Landsat image is shown in Fig. 22a where several icebergs are seen as bright objects south of Franz Josef Land. The combination of three channels in the Landsat image allows discrimination of sea ice (blue signature), clouds (yellow signature) and open water (dark signature). Note that icebergs located inside the area of thin clouds can also be identified, while icebergs inside the drifting sea ice cannot be detected because the signature of icebergs is similar to the sea ice signature. Iceberg A, B and C have size of 250m, 175m and 415 m, respectively. Fig 22 b shows the whole Landsat image with iceberg analysis, showing all icebergs that could be identified in the ice-free part of the image.
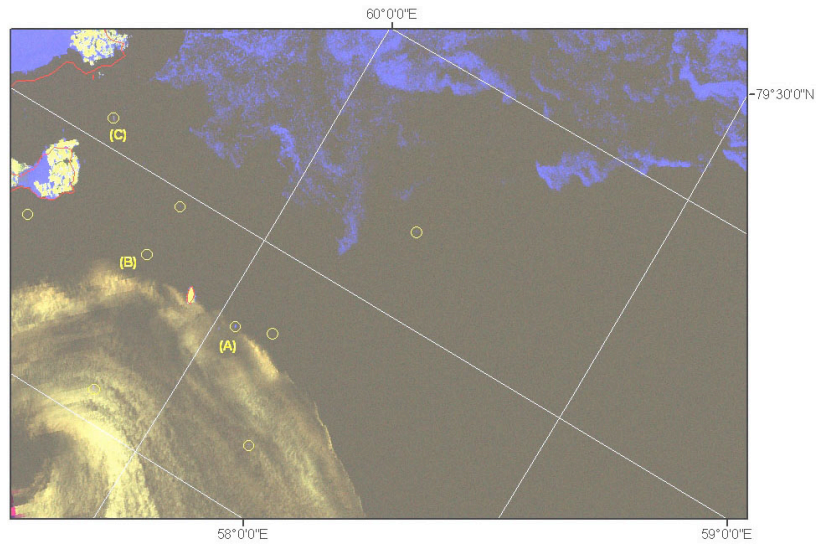
a
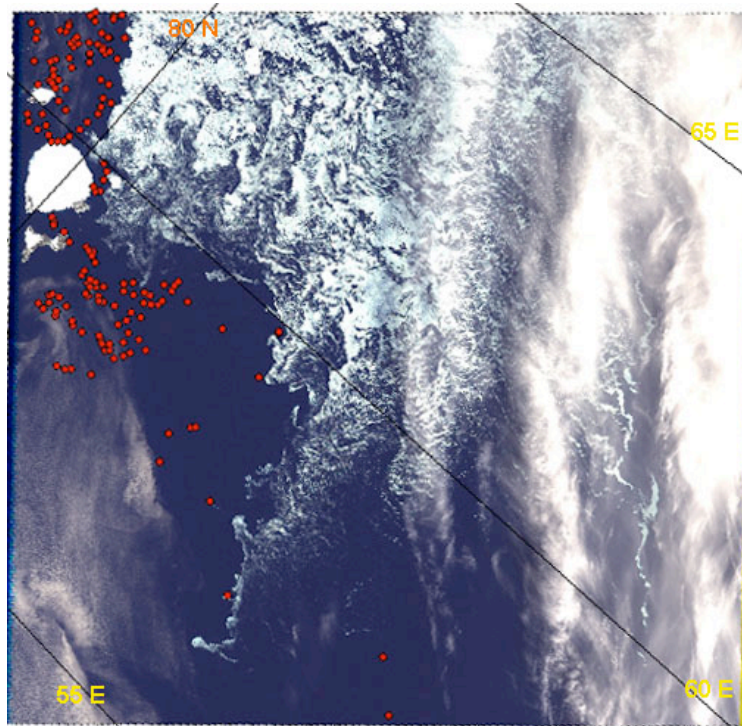
b

Figure 22. (a) Subset of Landsat image (27 July) south of Franz Josef land, showing icebergs in open water marked by circles. The blue areas in the upper part of the image is sea ice. (b) The full Landsat image with red dots showing all identified icebergs.

Another example of iceberg identification in open water half way between Franz Josef Land and Novaya Zemlya is shown in Fig. 23. A large part of this image is covered by thin, scattered clouds, making iceberg detection more difficult. By combining three channels in the Landsat image it is possible to discriminate between clouds (bright signature) and sea ice/icebergs with a more bluish signature. This method was used to identify three icebergs in the area with very scattered clouds, shown in the zoomed subimages on the right side in Fig. 23. These icebergs have size between 82 and 256 m, estimated by counting pixels. Most of the Landsat image had cloud cover appearing as bright signature in the image. This bright signature prevents effective iceberg detection.

(1) Location: 78.75 N, 57.67 E
Length: 100 m

(2) Location: 78.50 N, 56.19 E
Length: 256 m

(3) Location: 78.39 N, 56 E
Length: 82 m
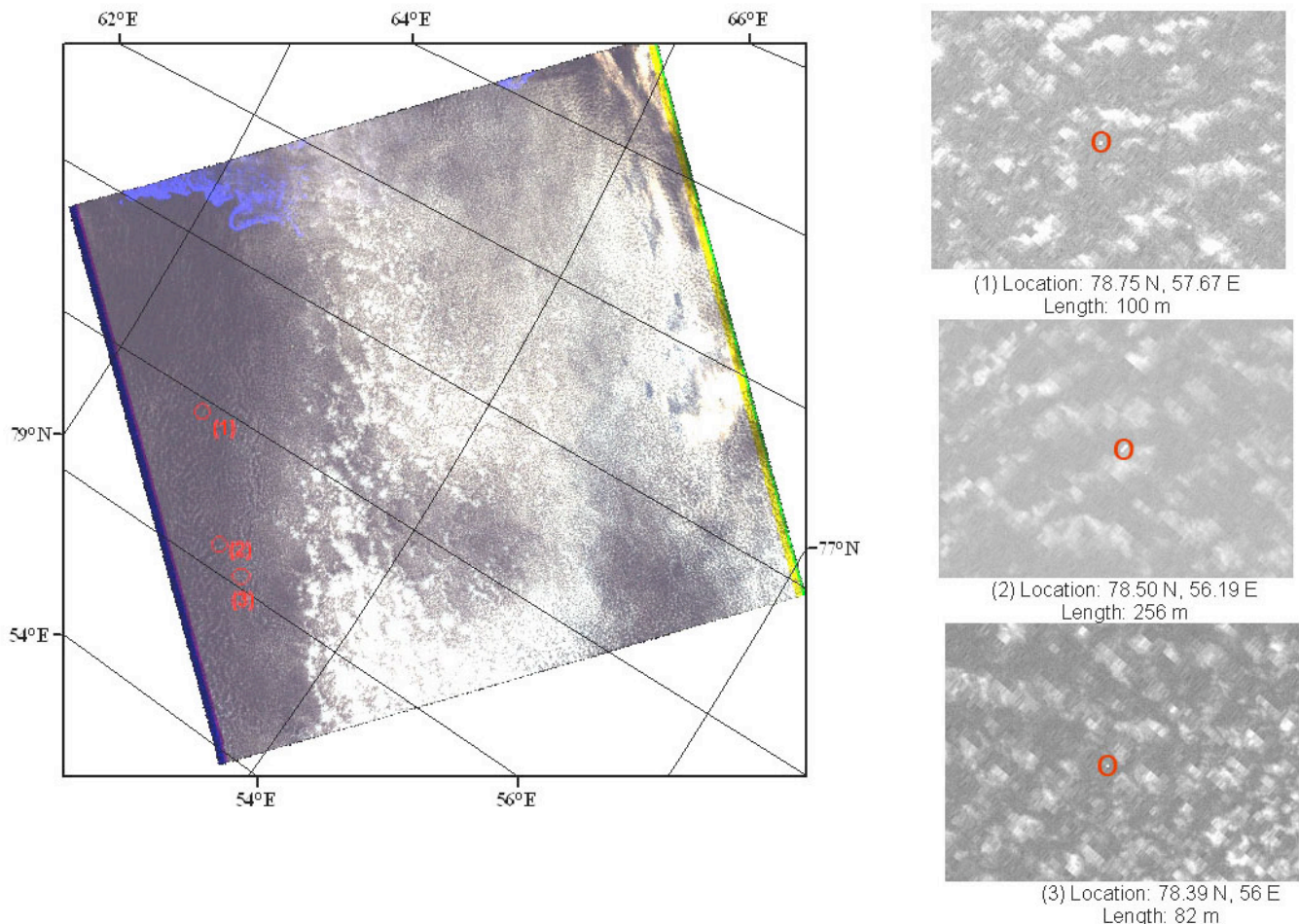
Figure 23. Landsat image (22 July) south of Franz Josef Land, showing three icebergs as bright objects, marked by the circles (left). Subsets of the images surrounding the icebergs are shown to the right. Note that the subimages are shown in panchromatic version (black and white), while the analysis used three channel combination where sea ice and icebergs appear with a bluish signature in contrast to clouds with a greyish signature.

In addition to the Landsat images, we also analysed a stripe of ASTER images from 22 June and compared it with Landsat image of the same area obtained about one month later (27 July). The ASTER image is presented in Fig. 24, showing that large parts of the fast ice around Salm Island and the adjacent islands are still present in June. Many icebergs are located in open water as well as in the fast ice. This situation was also observed in 2005 (Fig. 7), when many icebergs stayed in the area after the fast ice had disappeared.
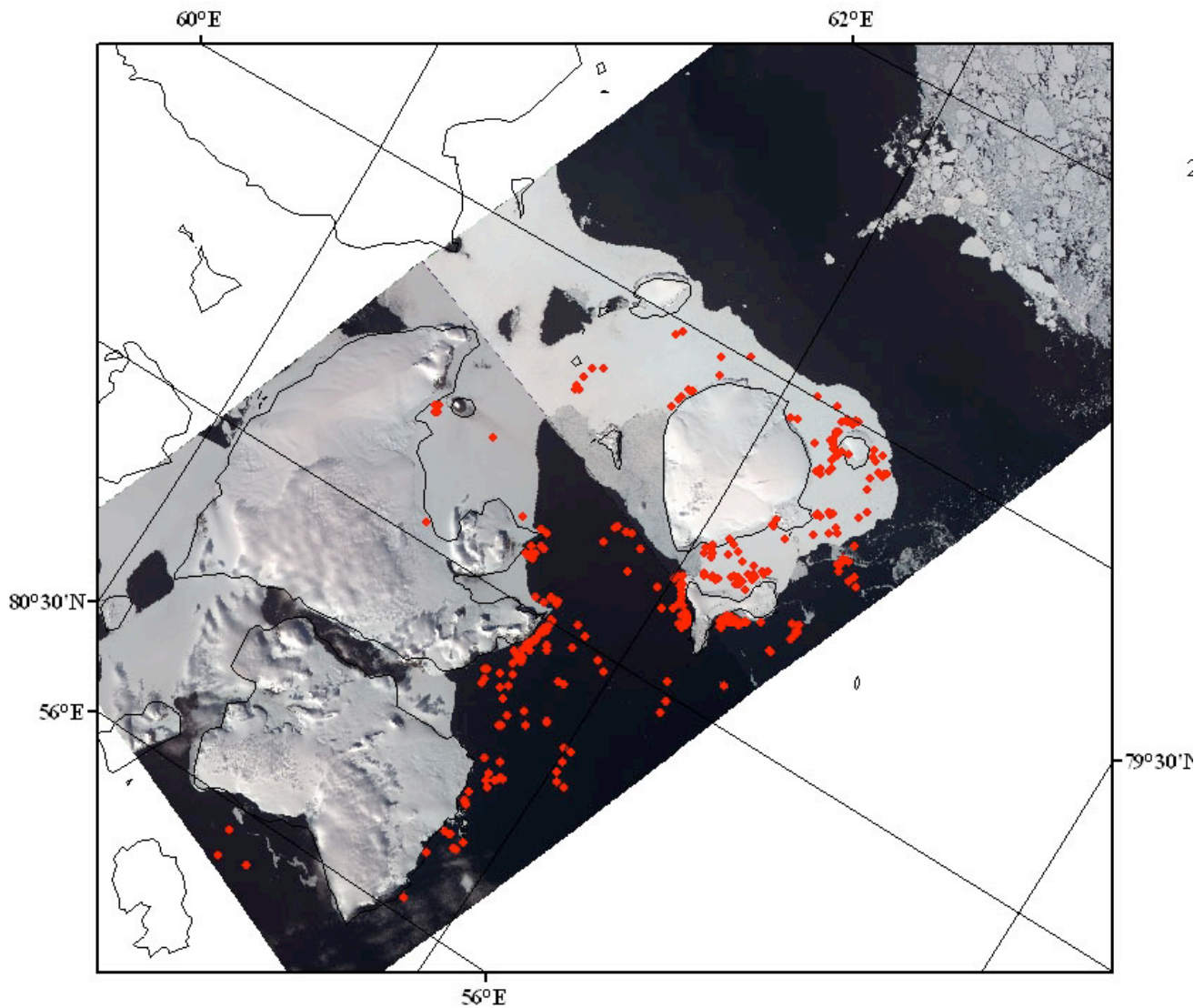
Figure 24. ASTER images from 22 June 2006, where icebergs identified in open water and in fast ice are shown by red dots.

The ASTER image from 22 June and Landsat image from 27 July covered the same area around Salm Island and could therefore be used to study the changes in sea ice as well as iceberg distribution over the 5-week period. The same sub-area in both images are presented in Fig. 25, showing that all the fast ice had disappeared during this period. All icebergs observed in the ASTER image are marked by red dots and all icebergs observed in the Landsat image are marked by green dots. A comparison of red and green dots shows the following:

- There are many more icebergs in the first image (>100) compared to the second (< 20), showing that a large number of icebergs have left the area in the period
- About 12 – 15 icebergs have moved to other positions within the images during the period, suggesting slow movement.
- About 5 – 6 icebergs have not changed their position, suggesting that they are grounded
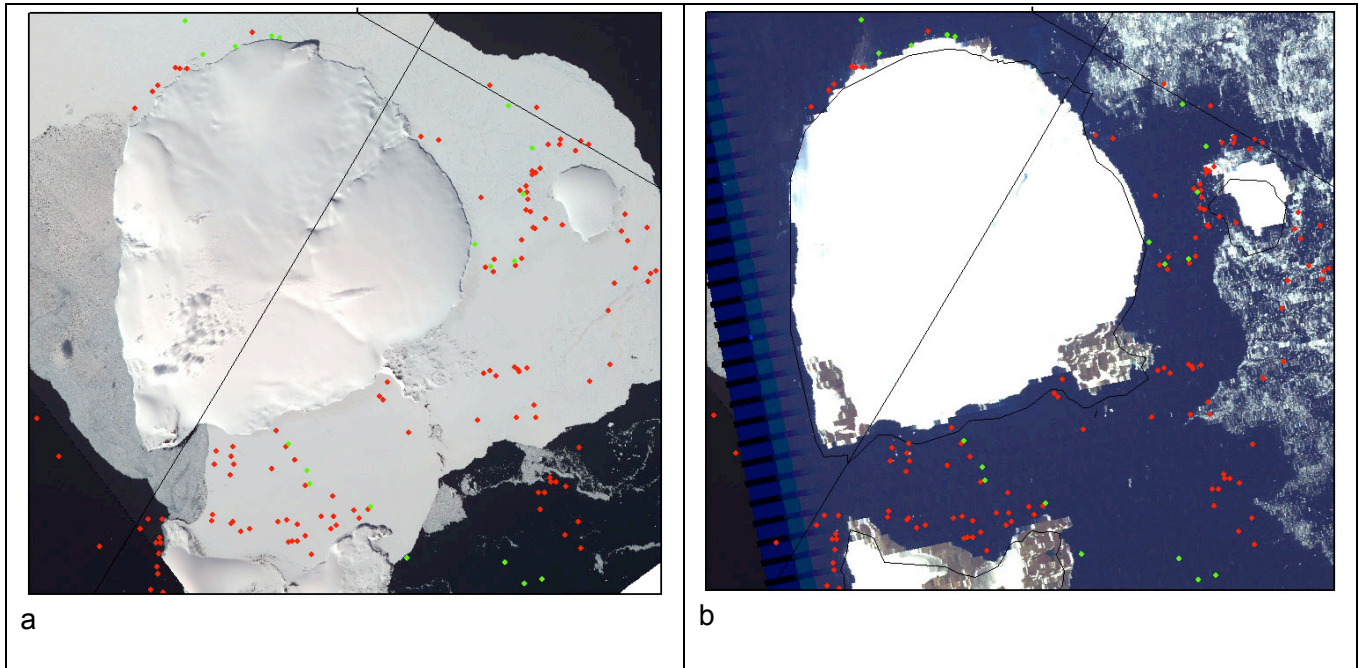
Figure 25. (a): Zoom-in of ASTER image from 22 June in of the area around Salm Island. (b): Zoom-in on the Landsat image of 27 July in the same area as the ASTER image. Red dots are icebergs in the ASTER image and the green dots are icebergs in the Landsat image.

Since the Salm Island area was investigated by Landsat images also in April 2006, it is possible to compare iceberg positions between 14 April and 27 July. We have compared the area south of Salm Island where it was observed that 3 – 4 icebergs were stationary from 22 June to 27 July. The area of comparison is shown in Fig. 26, where selected icebergs observed in the same position in both images are marked by circles. When the icebergs were found in exactly the same position, it means that they are grounded. It was straightforward to identify 8 icebergs that had not moved during the period of 3.5 months. If we had analysed other sub-areas we would probably have found more examples of grounded icebergs.

In chapter 3 and 4 we have presented a number of examples of how high-resolution optical images can be used to detect icebergs under different conditions and seasons. A major limitation in use of optical images is cloud cover and darkness. It is only feasible to use optical images in the period from April to September. In addition, it is also necessary to order full acquisition of images in order to secure that there are images on days with little cloud cover. The exercise to order continuous coverage of Landsat images for the whole summer season was very useful. We ended up with a limited amount of images of good quality, about 20, covering the period from March to August.

The next step in the study was to test the feasibility of using SAR images for iceberg detection. SAR is not hampered by cloud cover or darkness and can therefore deliver good quality images throughout the year. Several studies have been performed to assess the capability to use SAR for iceberg detection, but all the studies have shown that there are ambiguities in the detection. Since SAR images have speckle noise, it is very easy to misinterpret bright spots as icebergs. On this background we have performed a dedicated study where we have compared optical and SAR data for iceberg detection. This study is presented in chapter 5.
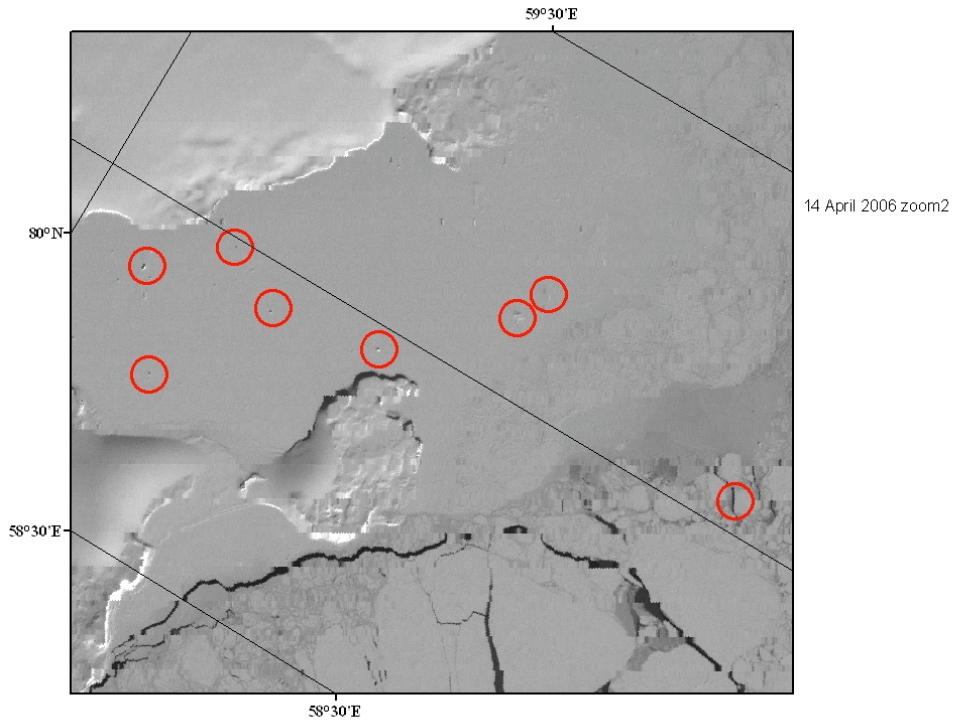
a
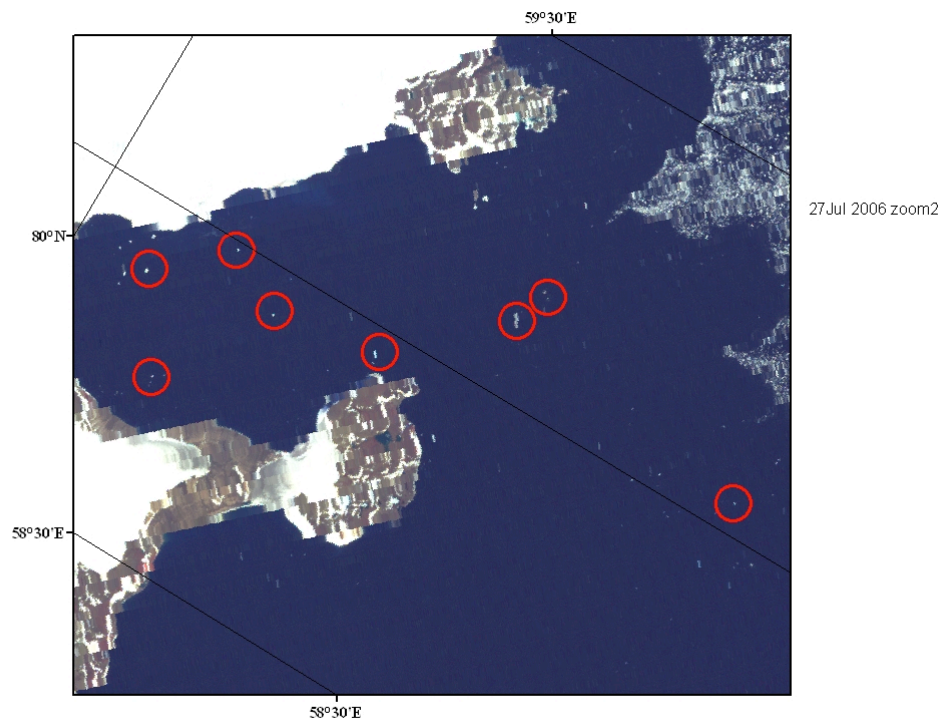
b

Figure 26. Comparison of iceberg locations on 14 April (upper image) and 27July (lower image) 2006 in the area south of Salm Island. The circles mark icebergs that are found in the same position in both images, showing that these icebergs are stationary.

5. Comparison of optical and ASAR alternating polarisation images

The overlapping area of the Landsat and the ASAR alternating polarisation image (Fig. 15) has been used to study iceberg detection in April 2006, with specific focus on detection capability in SAR images. The area around Salm Island was mainly covered by fastice in this period, and icebergs embedded in the fastice did not move between the SAR image acquisition (12 April) and the Landsat image (14 April). A selection of 15 icebergs of different size and shape were identified in the Landsat image (Fig. 27) and compared with signatures in the HH- and VV-polarisation images (Fig. 28). The detection criterion in optical images is that a bright object with a shadow on the northern side is an iceberg if located in fastice or in drifting ice. In fastice, the icebergs are not moving if the fastice is stationary. This allows repeated observations of the same icebergs in images taken with several weeks interval. In open water the dark shadow is not visible because the background is also dark. Icebergs located near land are often grounded, which can be confirmed by repeated observation in the same locations.
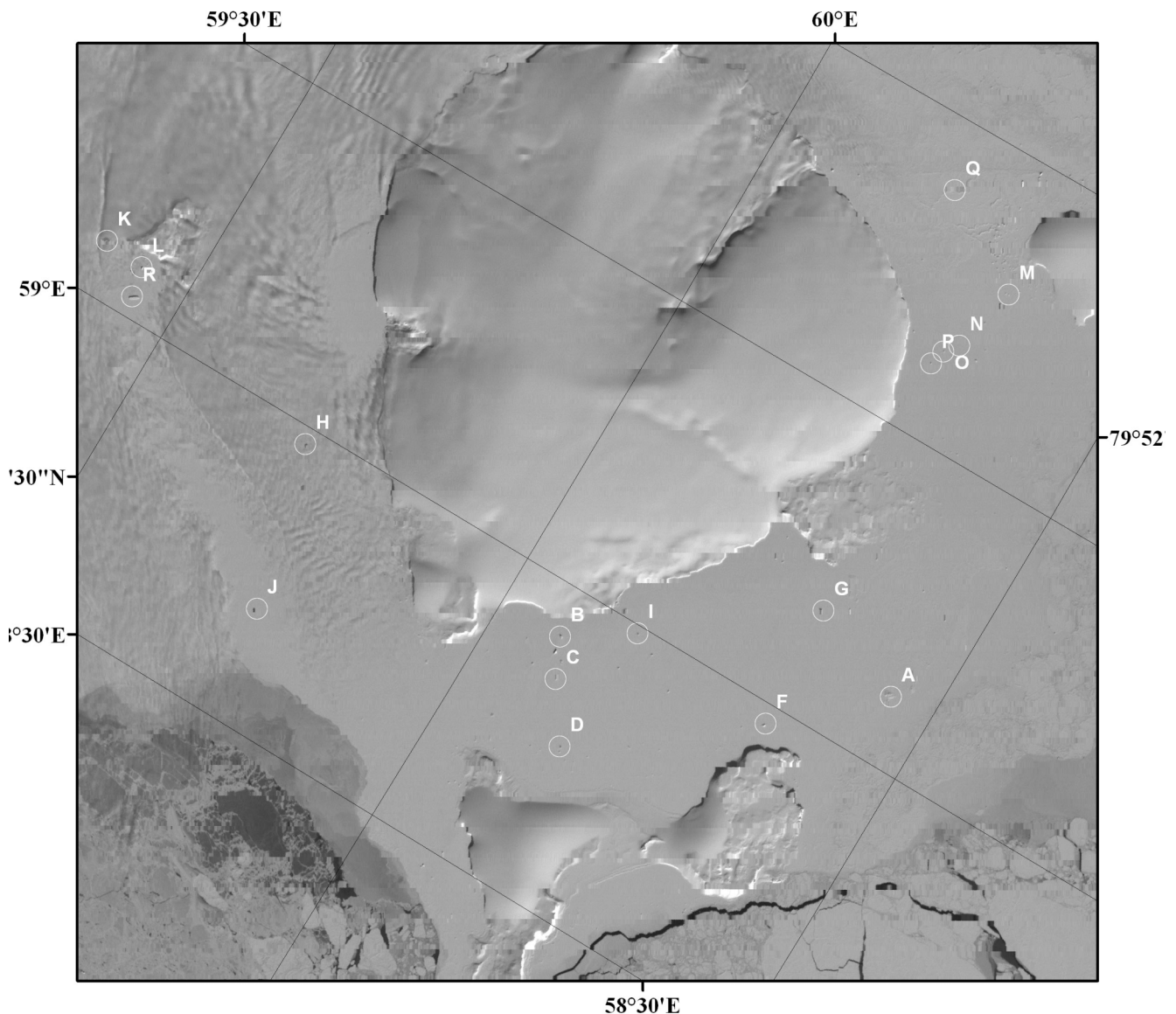
Figure 27. Subset of Landsat image from 14 April from the area around Salm Island with 15 identified icebergs (A to R). These icebergs were analyzed in the HH- and VV-polarisation images.
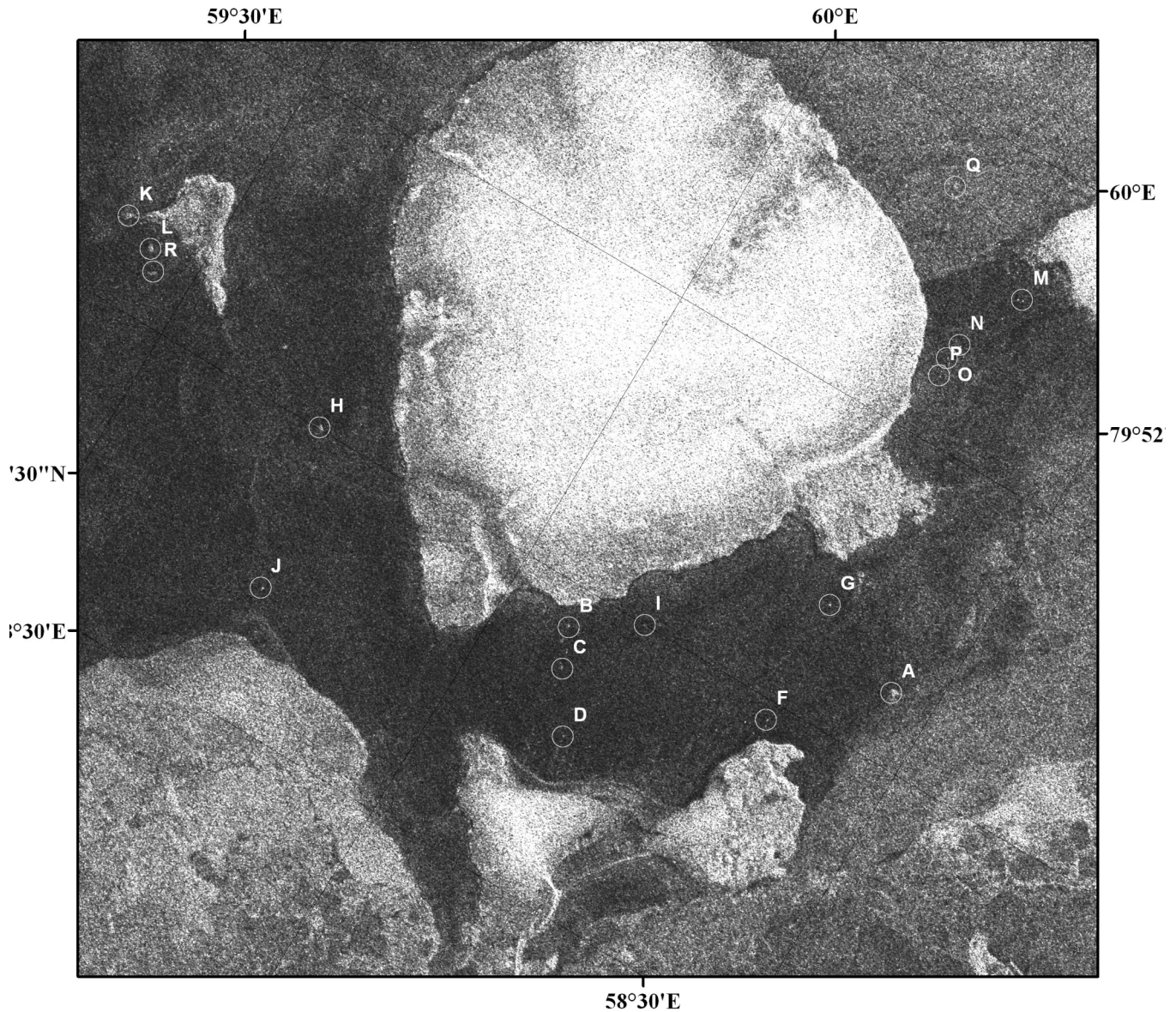
Figure 28. Subset of ASAR Alternating Polarisation (HH-Polarisation) image from 12 April from the area around Salm Island with the 15 icebergs identified in the Landsat image in Fig. 27.

The size of the 15 icebergs was determined from the number of pixels representing the iceberg objects in the Landsat image. The length varied between 50 and 400m, while the width varied from 30 to 230 m. 30 m is the smallest length scale that could be determined from images with pixel size of 15 m (Fig. 29). For each iceberg the mean and standard deviation of the pixel values identifying the iceberg object in the SAR images were determined and presented in Figs 30 – 33.

Fig. 30 presents the mean and standard deviation of the HH- and VV-backscatter of each iceberg. Some of the icebergs (e.g. M, N, O, P) are represented by only one pixel value and have therefore no standard deviation. The main results derived from Fig. 30 is that the backscatter is stable for both polarisations since standard deviation is much smaller that the mean. HH-polarisation is better than VV-polarisation because the latter shows weak or no signals for some of the icebergs. The size of the icebergs seems to have no direct impact on the backscatter. The shape of the icebergs, however, may have impact, as will be discussed later.
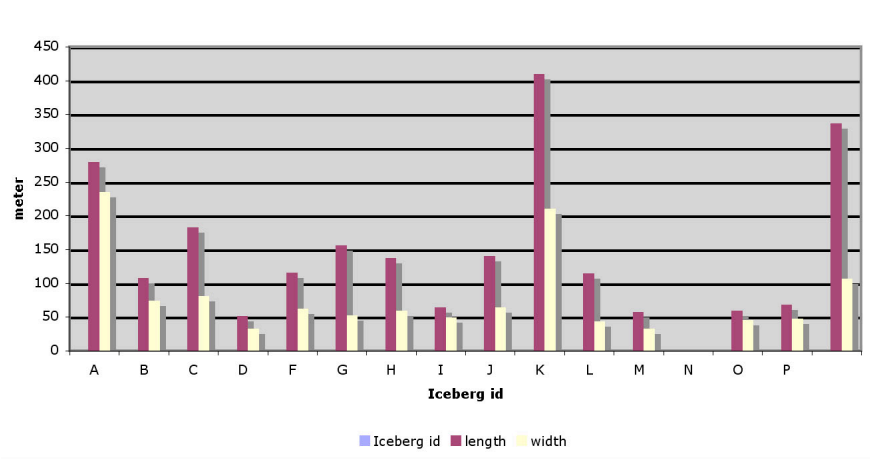
Figure 29. Length (red bars) and width (yellow bars) of the 15 selected icebergs, derived from the Landsat image.
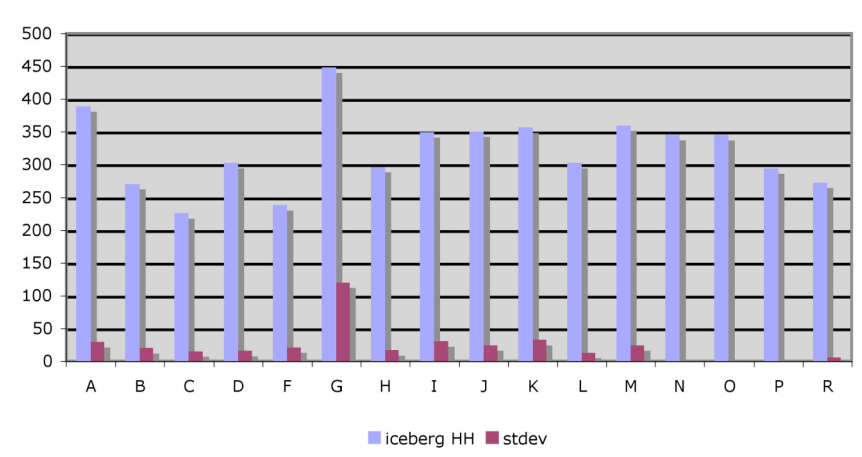
a
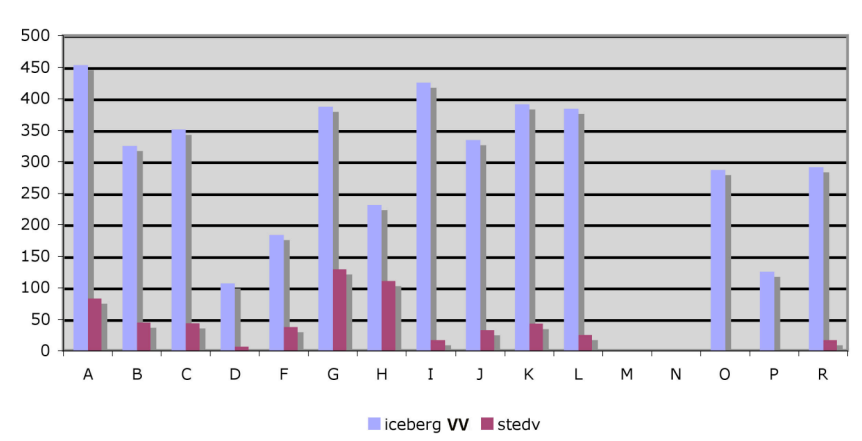
b

Figure 30. Backscatter from the iceberg objects A – R presented as mean (blue bars) and standard deviation (red bars) for HH-polarisation (a) and VV-polarisation (b). Some of the icebergs do not have a standard deviation because they were only represented by one pixel. Note that two icebergs (M, N) were only identified in HH-polarisation.

The mean backscatter is compared to the mean background signal for the fastice surrounding the icebergs (Fig. 31). The fastice in the study area is generally smooth, undeformed ice with low backscatter from both HH- and VV-polarisation. The smoothness of the fastice around the icebergs is documented in the Landsat image where ridges and other surface features appear as structures in the image. This was illustrated in the red and yellow polygons in Fig. 6.

The main result is that the mean backscatter of the icebergs compared to the background is generally higher for HH-polarisation compared to VV-polarisation. The HH backscatter is more stable, while the VV backscatter is more variable. For VV two icebergs could not be identified (M, N), while two others had a weak signal similar to the background (D, P).
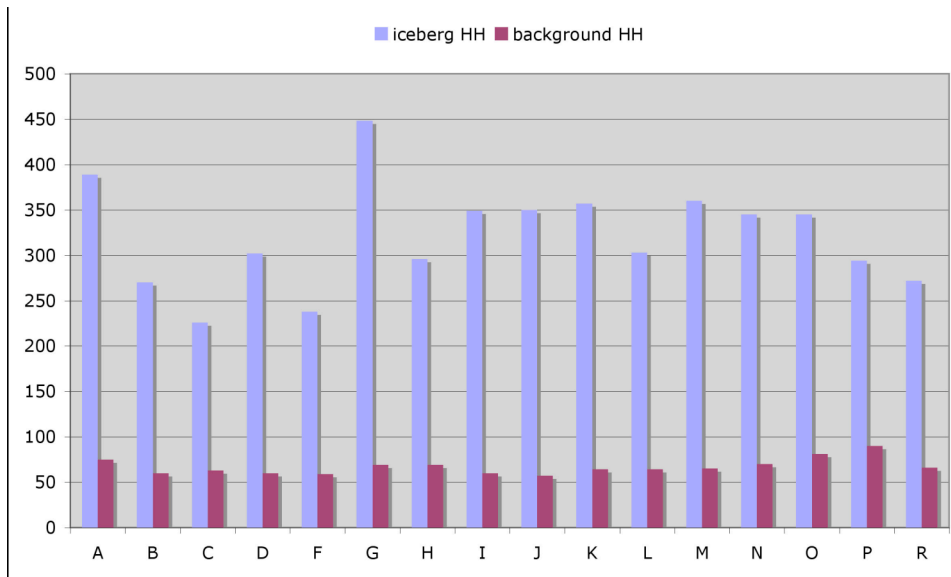
a
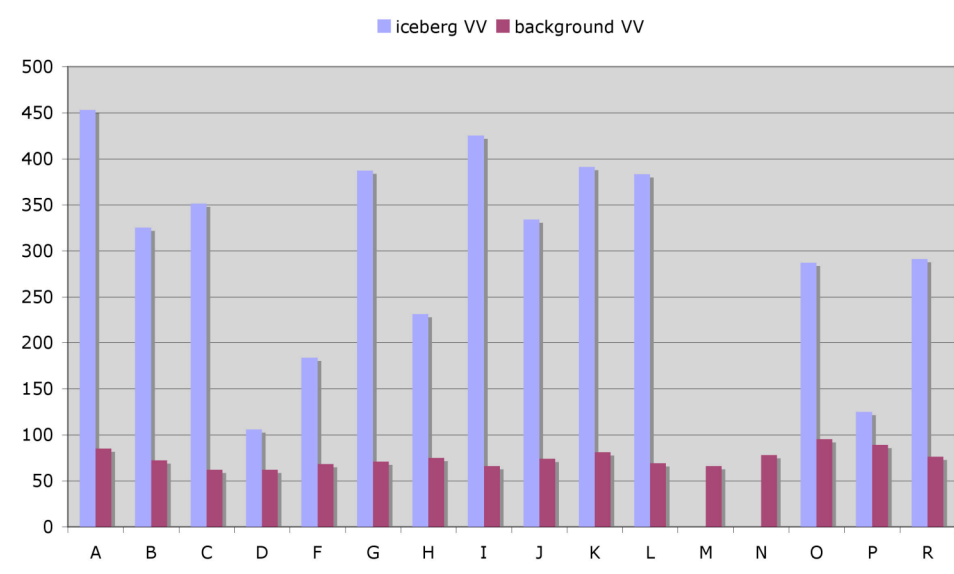
b

Figure 31. Iceberg backscatter (blue bars) compared to backscatter of the surrounding fastice (red bars) for HH-polarisation (a) and VV-polarisation (b). The digital values are provided by ESA when delivering the Alternating Polarisation data on CD.

The impact of iceberg shape and geometry on SAR backscatter could not be directly investigated because we did not have data on shape and size of the 15 icebergs. A first and simple approach to investigate the effect of iceberg geometry was to classify the icebergs into "simple and "complex" geometry based on information in the Landsat image. Icebergs were classified as "simple" if they appeared as single objects with bright signature and a corresponding object with dark signature representing the shadow. Examples of simple icebergs are F and P in Fig. 32 b. Icebergs were classified as complex if the object had several backscatter maxima or complex shadow pattern. Complex icebergs can represent clusters of icebergs grouped together or single icebergs with complex topography producing irregular shadows, as shown in A and B of Fig. 32 b.

The backscatter of the simple and complex icebergs were compared by taking the difference between the mean backscatter for HH and VV polarisation. The results show that for the simple icebergs HH had higher backscatter than VV, while for the complex icebergs VV was higher than HH (Fig. 32 a). Only one exception was found: iceberg I was classified as simple but VV was higher than HH. This is an interesting result, but it raises new questions and we cannot draw any conclusions at this stage. It is clear that more quantitative data on shape and geometry of icebergs is needed in order to study the effect on different SAR polarisations. Such study is needed to prepare for use of SAR in iceberg monitoring systems. New SAR satellites (RADARSAT-2, TerraSAR-X, Sentinel-1, etc.) will all have possibilities to select different polarisations (HH, VV, HV, VH), and for iceberg monitoring we need to know which polarisation is best suited for the task.
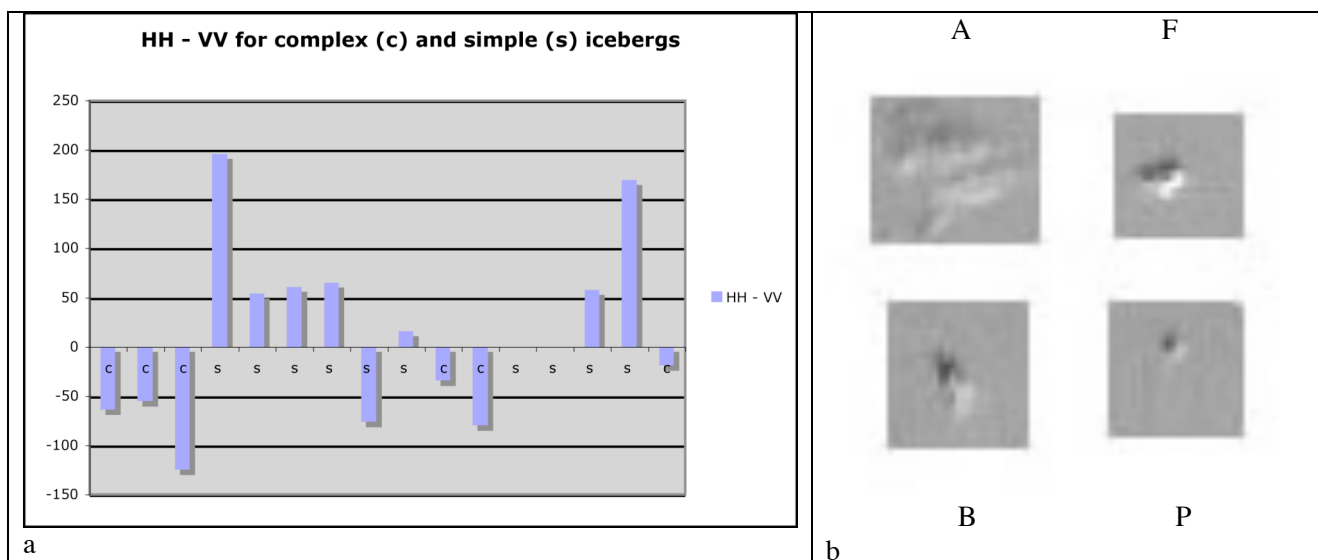
Figure 32. (a) difference between HH- and VV-polarisation for each iceberg and annotation of simple (s) and complex (c) geometry of the iceberg objects; (b) example of complex (A and B) and simple (F and P) iceberg geometry derived from Landsat zoom-in subimages.

In addition to ENVISAT Alternating Polarisation images, we also tested RADARSAT ScanSAR Narrow data, using the same 15 icebergs as described above. Since RADARSAT provides HH-polarisation, we compared the RADARSAT data with the ENVISAT HH data. To compare digital numbers from two different SAR systems, we calculated sigma-0 for both data sets, and presented sigma-0 for icebergs as well as for the background fastice. The results are shown in Fig. 33, where sigma-0 is presented in dB. Note that sigma-0 level is different between the two satellite images because the incidence angle is different. The lower backscatter level of the icebergs in the RADARSAT image (about -12 dB) compared to the ENVISAT image (about – 5 dB) is mainly due to the higher incidence angle of the RADARSAT data. The same situation is found for the background fastice (Fig. 33). Both SAR systems provide good contrast between iceberg signatures

and the background, which is a key criterion for detection. An exception is iceberg M, N, O and P which are detected only in the ENVISAT and not in the RADARSAT image. The pixel size of the RADARSAT image is twice that of ENVISAT (25 m versus 12.5 m), but size is not the main criteria for detection in SAR images. Icebergs M, N, O and P have size of about 50 m, but could not be detected in the RADARSAT image. Other icebergs with size of 50 m, such as D and I, were well detected in the RADARSAT image. The size of detectable targets in SAR images can be smaller than the pixel size. Detect ability in SAR images depends on geometry and orientation of reflecting planes of the target.
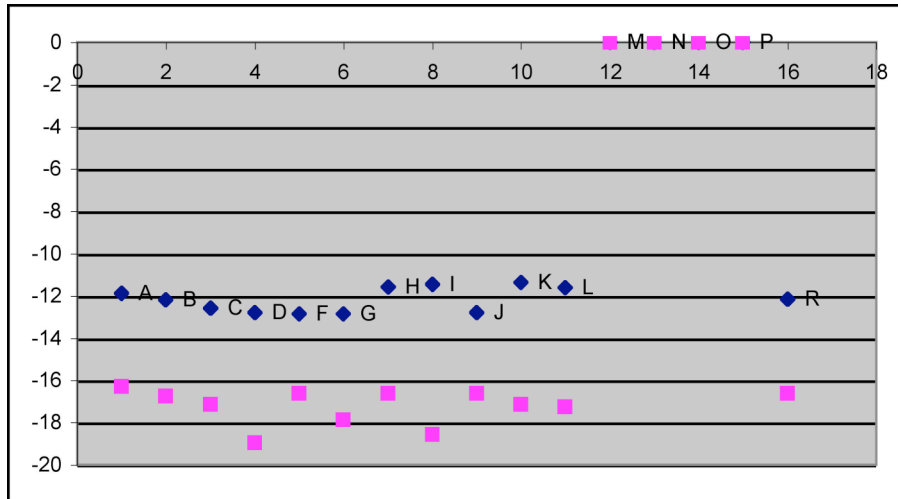
a
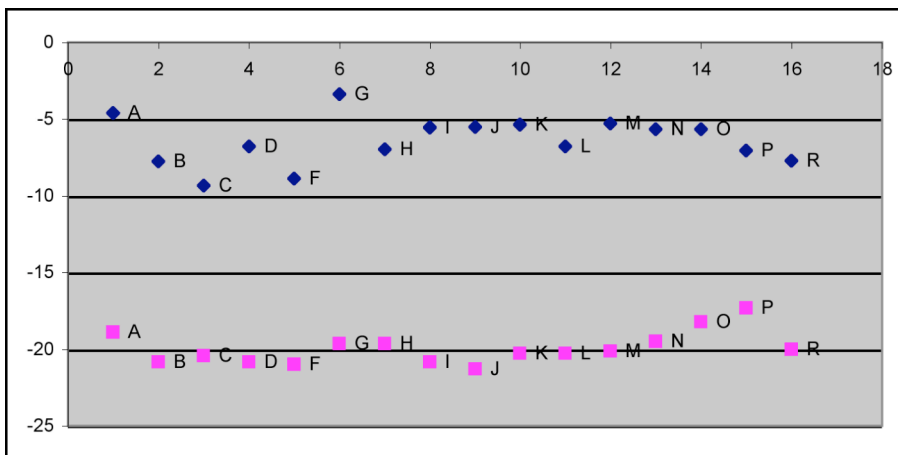
b

Figure 33. SAR backscatter (sigma-0) for the iceberg objects (blue dots) and the surrounding fastice (red dots) for RADARSAT ScanSAR HH-polarisation (a) and for ENVISAT HH-polarisation (b). The sigma-0 values are estimated for higher incidence angle for RADARSAT compared to ENVISAT. Also the pixel size is different: 25 m for RADARSAT and 12.5 m for ENVISAT Alternating Polarisation images.

The signatures of icebergs M, N, O and P were carefully compared between the Landsat and the ENVISAT HH-polarisation image (Fig. 34). M represents two very similar objects within the circle in both images. P and O represent well-defined icebergs in the centre of the circles in the Landsat image which can also be identified as bright spots in the SAR image. There are also other bright spots in the neighbourhood which cannot be recognised as icebergs. N was only observed in the

ENVISAT image and not in the Landsat image. N is therefore not included in the analysis presented in Figs. 29 – 31. N is assumed to be speckle noise producing many bright spots which are similar to the iceberg signature. The two subsets from Landsat and ENVISAT HH-polarisation image presented in Fig. 34 demonstrate very well that many bright spots in the SAR are not associated with icebergs. This has very severe impact on the use of SAR data for iceberg detection. Even if SAR images with pixels size of about 10 m can detect icebergs of size 50 m and more, the problem is the number of false detections. This study has only compared SAR and optical data for iceberg detection in fastice. Detection of icebergs in open water and in drifting ice has not been investigated as far as SAR data is concerned. More specific studies are needed to find solutions for more reliable iceberg detection in SAR images.
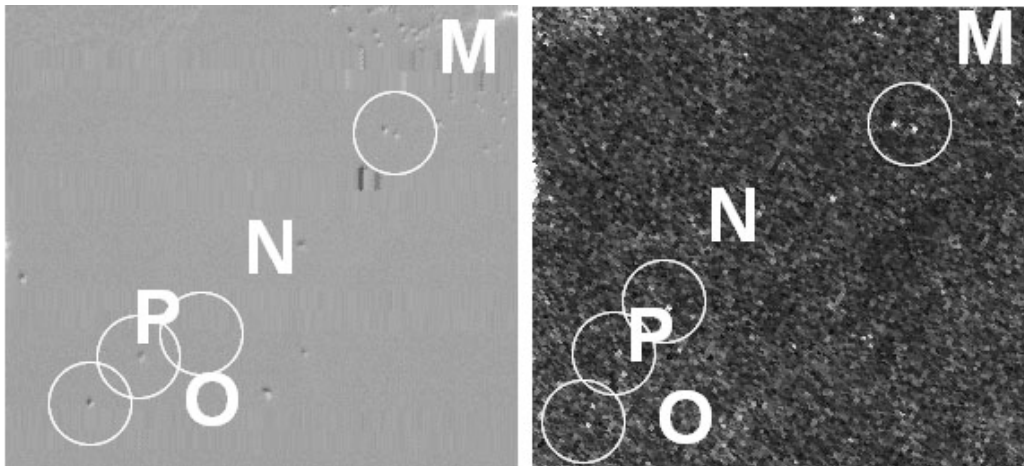
Figure 34. Subsets of Landsat image (left) and ASAR APP H-polarisation image (right) in the area where icebergs M, N, O and P were identified. These icebergs were not identified in the RADARSAT image. Note that N is not identified in the Landsat image, only in the SAR APP image. There are many more icebergs that can be identified in the Landsat image as well as in the SAR image. However, there are many more bright points in the SAR image which are not icebergs.

6. Summary of aircraft observations 1970-1989

Systematic monitoring of icebergs in the Arctic have been conducted by aircraft surveys in previous decades, and results of these monitoring projects were presented in several reports as part of the OKN IDAP project 1988 – 1994 (Spring, 1994). The present study is only a limited investigation of satellite remote sensing methods, and it is not directly comparable with the previous surveys conducted by repeated aircraft flight tracks. It is, however, useful to compare statistical estimates of iceberg probability from previous studies with new observations from satellites. Systematic observations by aircraft stopped in the 1990s, and new monitoring schemes for icebergs will need to use more satellite data.

An overview of the aircraft iceberg surveys in the Barents and Kara Sea conducted by Arctic and Antarctic Research Institute in the period 1970 – 1989 has been provided by Abramov and Zubakin (1992). This report shows that more than 1500 flights were conducted in the 20 year period and icebergs were observed in more than 1000 of the flights. The flight tracks are shown in Fig. 35. More than 16000 icebergs were observed in total and the annual and monthly distribution of the observations are presented in Table 2. In addition to this report, the Iceberg Atlas for the Arctic by Abramov (1996) gives the best overview of icebergs from early 1900 and up to about 1993.

Table 2: Number of icebergs and aircraft surveys 1970-1989 (Abramov and Zubakin, 1992)

Year	Jan		Feb		Mar		April		May		June		July		Aug		Sept		Oct		Nov		Dec		Σ obs	Σ flights
1970	0	0	1	1	0	0	7	3	90	8	49	11	6	6	150	16	847	23	231	12	0	0	0	0	1381	80
1971	0	0	52	7	401	9	226	9	97	7	122	13	85	11	59	13	151	12	70	11	4	2	0	0	1267	94
1972	0	0	25	4	42	5	243	10	70	10	89	16	70	14	235	17	210	9	5	5	3	1	0	0	992	91
1973	0	0	18	4	24	3	4	1	46	5	49	7	96	12	332	9	323	13	26	6	0	0	0	0	918	60
1974	0	0	0	0	0	0	102	4	0	0	0	0	2	2	22	12	65	12	27	10	6	2	0	0	224	42
1975	0	0	11	2	55	9	64	2	119	5	0	0	0	0	9	1	31	12	0	0	0	0	0	0	289	31
1976	0	0	12	1	12	1	53	2	70	10	62	4	81	8	269	12	232	12	48	5	0	0	0	0	839	55
1977	0	0	4	1	82	5	31	6	52	5	16	4	66	7	50	10	72	16	36	5	15	3	0	0	424	62
1978	0	0	8	4	54	2	162	8	54	4	15	4	9	2	105	7	119	11	41	7	0	0	0	0	567	49
1979	0	0	20	4	11	5	261	8	306	8	9	2	15	5	184	9	125	5	65	6	3	1	11	2	1010	55
1980	0	0	5	3	19	3	177	6	22	3	219	8	4	1	1	1	48	6	26	3	72	4	0	0	593	38
1981	8	2	10	3	15	3	21	2	0	0	14	4	2	1	39	4	33	6	27	6	4	1	0	0	173	32
1982	0	0	8	2	15	4	46	6	55	3	31	3	22	5	25	3	28	2	5	3	0	0	0	0	235	31
1983	1	1	0	0	12	4	13	6	60	5	8	3	52	6	154	10	888	10	69	2	0	0	0	0	1257	47
1984	0	0	141	8	378	13	141	11	142	10	24	5	72	3	367	8	188	4	31	1	8	3	0	0	1492	66
1985	0	0	20	5	293	16	186	6	263	2	0	0	33	6	93	8	300	5	107	5	2	2	1	1	1298	56
1986	2	1	14	4	15	5	314	7	32	3	27	5	45	4	55	2	393	4	11	4	40	1	1	1	949	41
1987	0	0	23	6	25	4	107	6	1	1	0	0	0	0	186	11	68	4	0	0	0	0	0	0	410	32
1988	1	1	12	3	62	5	14	5	1	1	0	0	0	0	192	3	4	3	43	5	0	0	0	0	329	26
1989	0	0	10	4	0	0	0	0	70	1	679	4	4	1	0	0	379	7	401	8	0	0	10	2	1553	27
Σ obs	12		394		1515		2172		1550		1413		664		2527		4504		1269		157		23		16200	
Σflights		5		66		96		108		91		93		94		156		176		104		20		6			1015

The aircraft surveys were normally performed at a flight altitude between 100 and 500 m, with an observing range of 20 – 30 nautical miles. A main question is how large part of the icebergs are captured by this observing scheme. It is obvious that large parts of the areas that potentially can

have icebergs are not covered by the surveys. The data presented in Table 2 is underestimating the total amount of icebergs, and the question is by how much. Another issue is the size distribution of the icebergs. Previous investigations show that most of the icebergs in the Barents Sea have size less than 100 m (Fig. 36). This has impact on the detection capability using aircraft surveys as well as satellite observations.
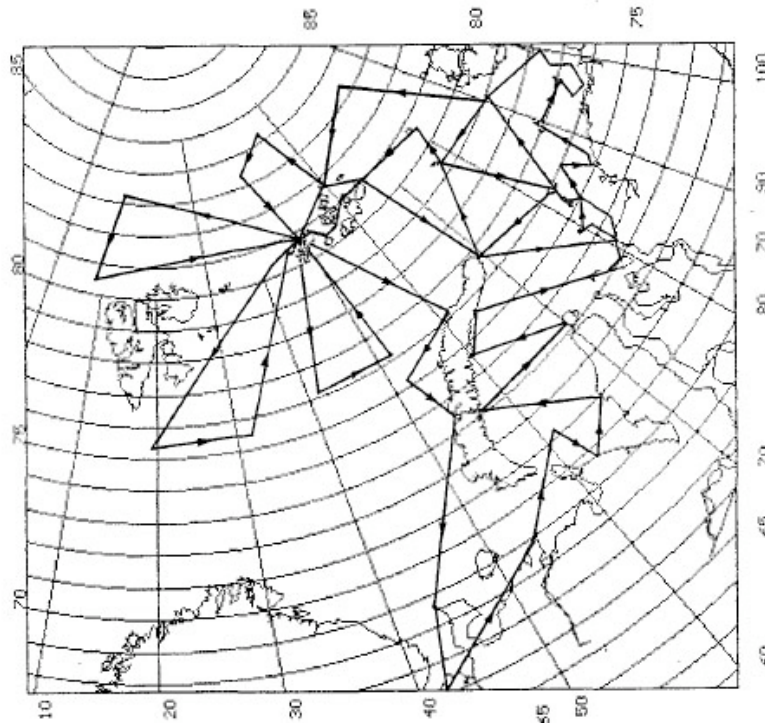
Figure 35. Map of standard aircraft flight tracks used for icebergs surveys 1970 – 1989 (Abramov and Zubakin, 1992).
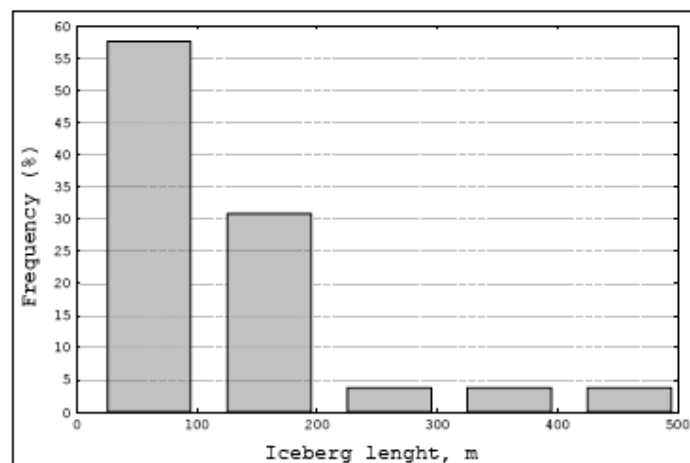
Figure 36. Iceberg size distribution in the Barents Sea (Zubakin et al., 2004).

As observed in Table 2 and Fig. 37a, the number flights and consequently the number of icebergs were at a minimum in the dark winter month November, December, January and February.

Maximum observations in the winter season was in April, while summer observations were at maximum in August and September. Fig 37b shows the annual variability in total number of observed icebergs. There are noteworthy minima in 1974-75, 1981-82, and 1987-88. These minima are correlated with lower number of survey flights. Therefore the sampling issue is important, so we have made comparisons between number of observations and number of survey flights.
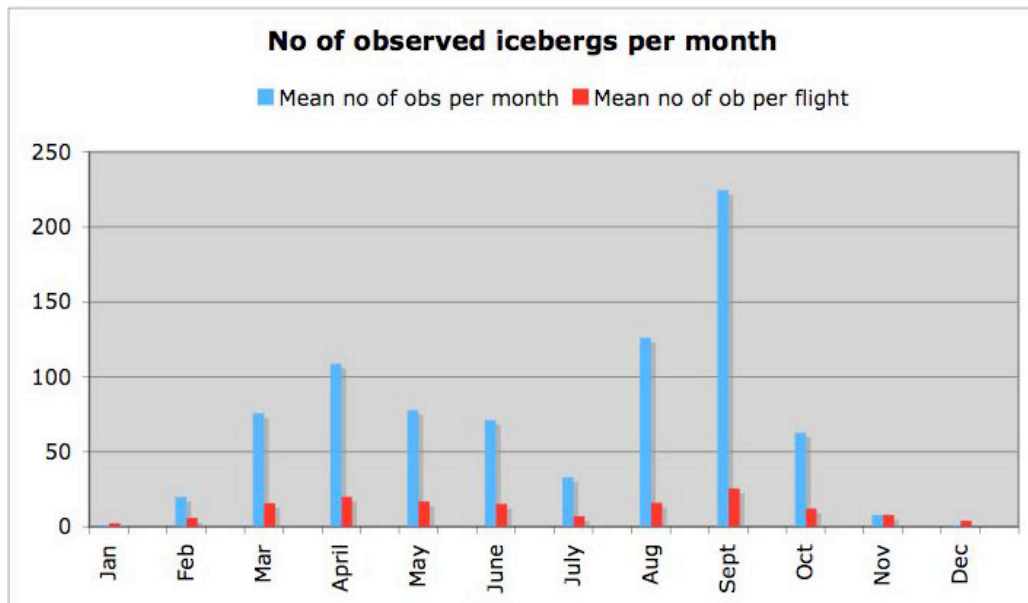
a
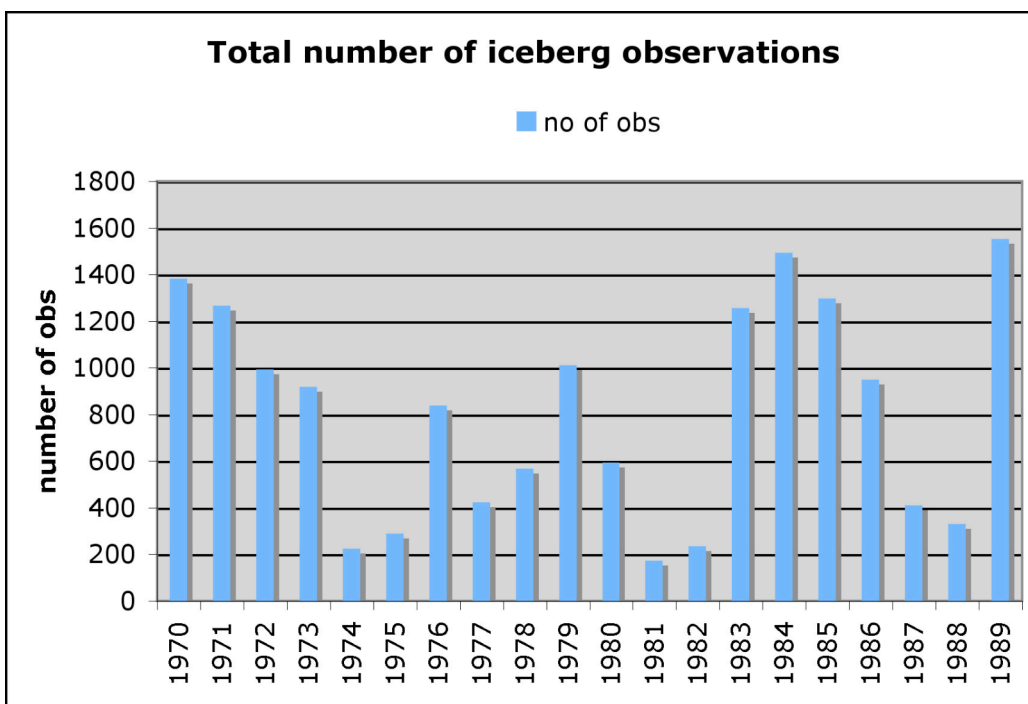
b

Figure 37. (a) Mean number of observed icebergs per month (blue bars) and mean number of observations per flight (red bars), (b) Total number of observed icebergs per year.

Figure 38a shows total number of flights and number of observed icebergs per flight for each year. It is noteworthy that the years with lowest number of observed icebergs in Fig 37b (1974-75, 1981-82 and 1987-88) also have the lowest number of flights. In addition, 1974, 1981 and 1982 had the lowest number of observations per flight. 1989 is remarkable because the number of observations per flight is significantly higher than all the other years. By comparing total number of flights with total number of observed icebergs (Fig. 38b) is possible to assess if there has been a trend in iceberg occurrence over the 20 year period. The years 1970-73 is characterised by high number of observations and high number of flights. If we compare this with the next period of high number of observations (1983-1986), we see that relatively more icebergs were observed by a lower number of flights. Except for the extreme year 1989, it can be concluded that iceberg occurrence in the survey area showed large interannual variability and this variability is to a large extent correlated with the number of flights.

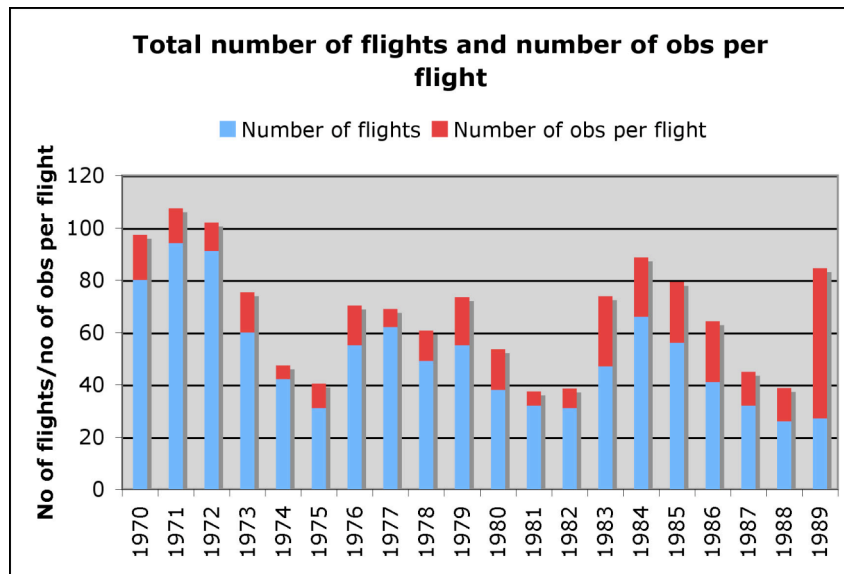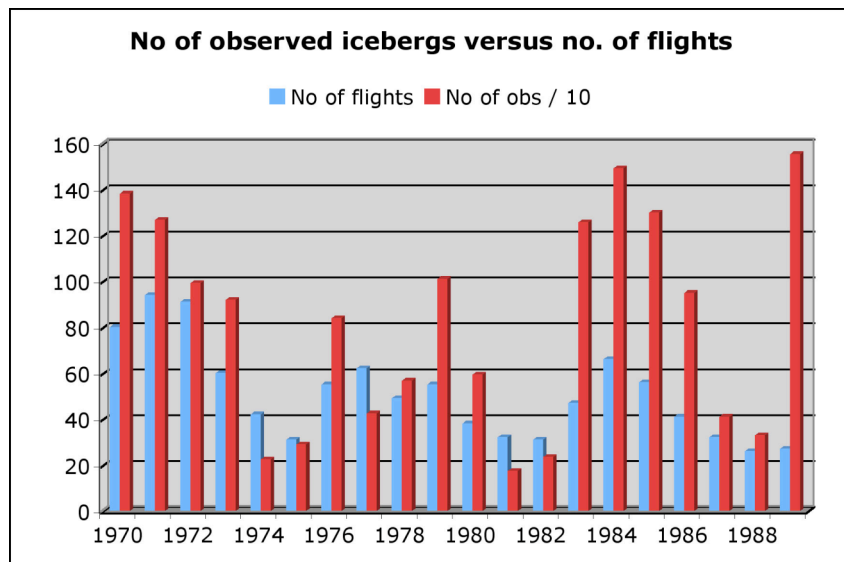
a

b

Figure 38. (a) Total number of survey flights per year (blue bars) and total number of observations per flight (red bars); (b) total number of observed icebergs, divided by ten (red bars) compared to total number of flights (blue bars).

The observations of icebergs from aircraft surveys have been used to produce iceberg distribution maps. The ice probability maps shown in Fig. 39 are examples of the monthly maps provided by Abramov and Zubakin (1992). A more extensive compilation of iceberg data have been published in the Atlas of Arctic Icebergs by Abramov (1996).
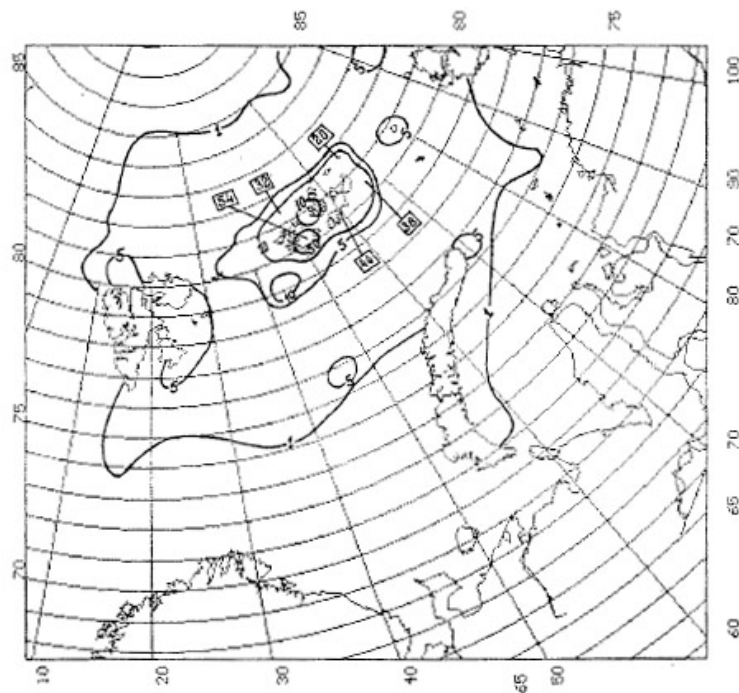
a
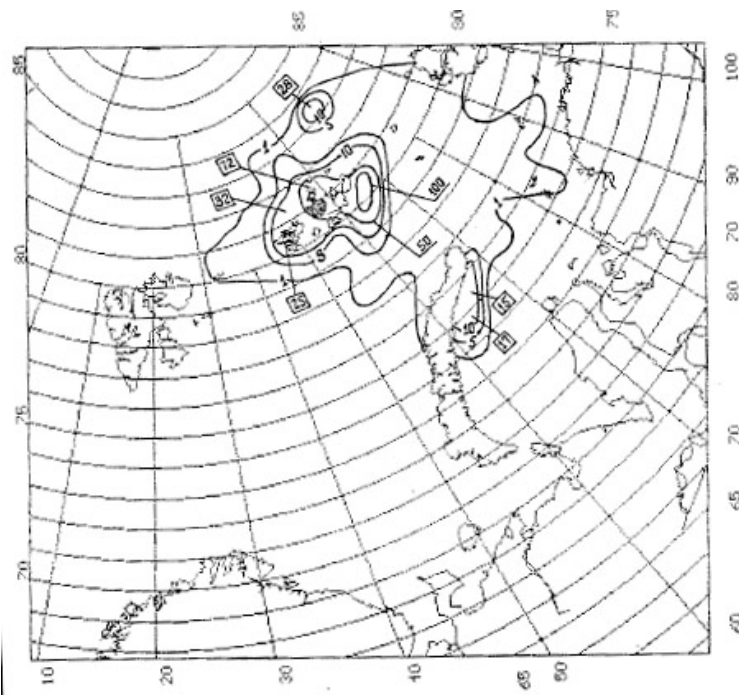
b

Figure 39. Iceberg concentration maps for (a) April and (b) September from Abramov and Zubakin (1992). The isolines represent maximum number of icebergs per 10000 km².

The variability of the southern iceberg extent in different parts of the Arctic Ocean has been reviewed in the Iceberg Atlas (Abramov, 1996). For the Barents Sea, observations are available from early 1900 and scattered data are also available from the 1800. Regular observations started to be collected in the 1930s, and annual southern border of icebergs in the Barents Sea are shown in Fig. 40.
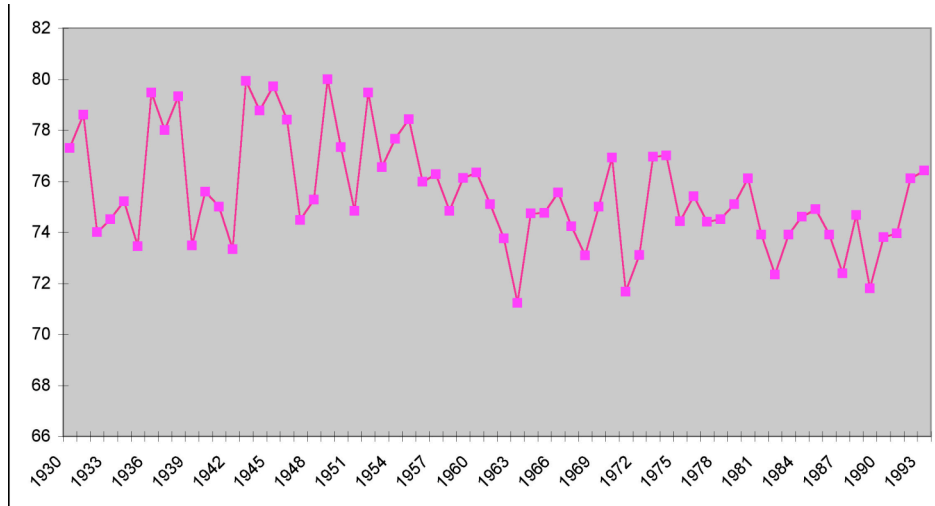
Figure 40. Southern extent of icebergs in the Barents Sea from 1930 to 1993 (Abramov, 1996). The y-axis shows latitude.

The iceberg observations were less systematic before the 1930s when regular aircraft surveys started. Russian observations in the Eastern Barents started in 1881 and Zubakin (2004) has presented a cumulative map of iceberg occurrence in this region in Fig. 41 a.
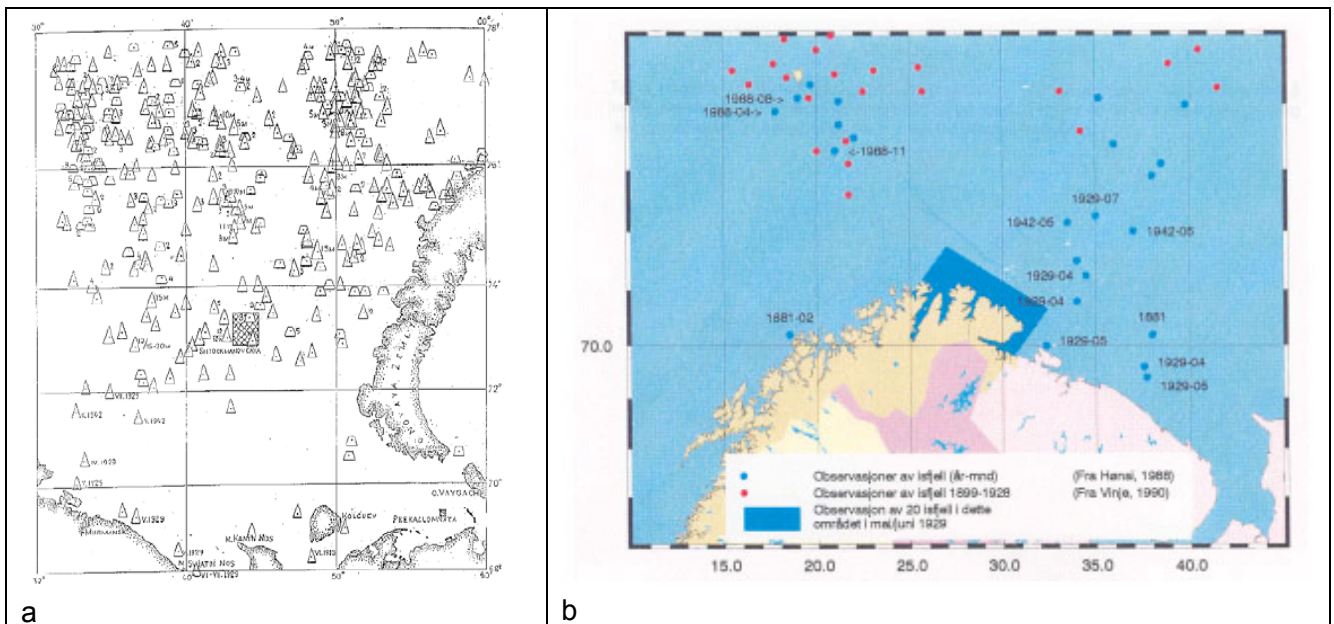
Figure 41. (a) iceberg occurrence in southern and eastern Barents Sea from 1881 – 1993 (from Zubakin, 2004); (b) iceberg observations in Norwegian part of the Barents Sea (from Hønsi 1988).

Observations in the Norwegian part of the Barents Sea also goes back to 1800. Report have been provided by Hønsi (1988) and Kvitrud and Hønsi (1990) showing that:

- The first report of icebergs in the Barents Sea south of 74°N is in February 1881. Two icebergs reached the coast at Kvaløya in Troms at 70°13'N 19°30'E. The larger iceberg of the two was 7 metres high.

- In June 1881 several icebergs were observed at Gamvik, Berlevåg and Syltefjord at East-Finnmark. The largest iceberg was enormous, with a length said to be 10 km, and a sail height of 30 m.

- During the period of April-June 1929, a number of icebergs reached the coast of Kola Peninsula and eastern Finnmark (Fig. 41 b). The local newspapers in Finnmark reported that they reached up to 30 metres above sea level

- In 1939 two icebergs were observed at Koi- fjorden close to Gamvik.

In May 2003, surprisingly many icebergs were observed in the Shtokman area south to 72 N (Zubakin et al., 2004). From ship radar observations, 109 iceberg and bergy bits were found in the area between 71 and 75 N and between 40 and 46 E. The largest iceberg was 190 by 430 m. Before this event, the iceberg occurrence probability for the Shtokman area was that 7 icebergs would occur once in ten years. After May 2003 this probability rose to 19 icebergs occurring once in ten years. By looking at Fig. 40, we can see that icebergs reaching down to 72 N also occurred in 1989, 1971 and 1963. Before that extreme iceberg extents occurred in 1939, 1929 and 1881, as described above.

Since the iceberg distribution can vary strongly from year to year, it is important to have good monitoring and tracking systems for the icebergs. Extreme events can happen fro year to year and there is no direct method to predict when icebergs will extend far south in the Barents Sea.

7. Conclusions and recommendation for further work

The most important sources of icebergs in the Barents Sea are the glaciers in Franz Josef Land followed by northern Novaya Zemlya and Nordaustlandet in Svalbard. In recent years the icebergs in this region have become increasingly important because of the growing oil and gas exploration in the Arctic. It is a real challenge to observe and quantify the icebergs in the Barents Sea, because they are generally small (< 100 m), they are to a large extent embedded in sea ice, and there is no regular monitoring system for icebergs in the region. Systematic observations of icebergs by Russian aircraft surveys, which started in the 1930s, stopped in the early 1990s. In the last 15 years only research expeditions have been carried out without possibility to monitor icebergs over large areas. Hence our knowledge of iceberg frequency and distribution in recent years is quite limited. It is not realistic that the extensive aircraft monitoring programme from previous decades will be resumed. In the future, it is therefore necessary to use more satellite data in iceberg monitoring.

Use of satellite images has been investigated in the last two decades but the resolution and coverage of the images used so far has not been sufficient for monitoring icebergs, except for the largest icebergs (> 100 m). In the Barents Sea 55 % of the icebergs are less than 100 m in horizontal extent, and with present satellite data we have shown that icebergs down to 50 m can be observed from satellites.

In this study we have focused on the following activities:

(1) Search in satellite data archives for high-resolution optical and SAR images that are co-located with previous field observations, especially in the IDAP period (1988 -1994) when extensive field observations of icebergs were conducted. We were searching for Landsat, SPOT and ERS-1 SAR images, but very limited data sets form these satellites were found for the IDAP period and subsequent years until about 2004. In the last 2 – 3 years, high-resolution optical images from Terra ASTER have started to be produced in glacier and coastal regions, including Franz Josef Land and Novaya Zemlya. Because of available ASTER images and field observations from recent AARI expeditions, we have focused the study on acquisition and analysis of data for 2005 and 2006.

(2) In 2005, we obtained and analyzed about 10 good quality ASTER images that were collocated with observations performed by AARI during April using ice-going vessel "Somov" with helicopter. The ASTER images were analysed for icebergs in two areas: south of Salm Island in Franz Josef Land and off the northwestern coast of Novaya Zemlya. The ASTER images have a pixel size of 15 m and cover 60 by 60 km each. South of Franz Josef Land about 250 icebergs were found in three images, while about 50 icebergs were found off the coast of Novaya Zemlya in five images. Some of the icebergs found in the ASTER images were confirmed by the in situ observations from Somov. Detailed validation of the size and shape of the icebergs was not done because we did not have such data from the Somov expedition. We also checked the time variability of the iceberg population near Salm Island between 20 April and 18 June. We found that the icebergs had changed very little in this period. Also the fast ice where most of the icebergs were embedded changed little during this period.

(3) In 2006 we had the possibility to pre-order satellite images for the specific study areas. We ordered acquisition of Landsat and ASTER optical images, each covering 180 by 180 km, and ENVISAT ASAR images with alternating polarisation and high resolution (pixel size of 12.5 by 12.5 m). We also had access to RADARSAT and ENVISAT wideswath images with coarser resolution

that were used to compare with the high-resolution optical and alternating polarisation SAR images. The main period was April, when AARI conducted field observations with Somov, similar to the experiment in 2005. Analysis of the optical images resulted in detection of several hundred icebergs south of Franz Josef Land (in one Landsat image) and about 100 on the coast of Novaya Zemlya (in one Landsat and two ASTER images). The acquisition and analysis of optical images continued through the summer months, showing the presence of many icebergs south of Franz Josef Land in late July. The data coverage did not allow us to estimate changes in iceberg populations in the whole northeastern Barents Sea during the summer months. But we could check the changes in iceberg distribution near Salm Island from April to late July. This study showed that most of the icebergs embedded in the fastice stayed in the area until the end of June when the fastice was still present. Similar results were found in 2005. During July, the fastice disappeared and so did most of the icebergs around Salm Island. However, about 20 icebergs stayed in the same position after the fastice had disappeared, suggesting that they were grounded or had moved very slowly during July.

(4) Mapping the northeastern Barents Sea as a supplement to aircraft survey on 27 July. It was attempted to search for icebergs with satellite data from the Shtokman area in the north-eastern part of the Barents Sea. For this reason Landsat images were ordered for every orbit covering this region in June, July and August. Images with good quality were checked and downloaded from the Landsat archive. About 10 landsat images were analysed and icebergs were only found in the northeaster part, as described in section 4.2. We also prepared for ordering SPOT images, but we did not use any because the cost was relatively high. SPOT has a better spatial coverage compared to Landsat because there are three satellites in operation, giving us possibility to get better data coverage of the study area.

(5) Study of SAR detection capability and comparison with optical images. A dedicated study on iceberg detection capabilities in ENVISAT ASAR alternating polarisation images was performed including comparison with Landsat optical images in April 2006. SAR images with both HH- and VV-polarisation and higher resolution compared to the standard wideswath images offer a better possibility to test SAR systems which will be available in near future (e.g. RADARSAT-2, TerraSAR-X). 15 icebergs of size from 50 to 400 m were identified both in the Landsat panchromatic image (pixel size 12.5 m). The HH image could identify all 15 icebergs, while the VV-images failed to identify 4 of the icebergs that had a size of about 50 m.   The geometry of the icebergs were not observed in situ, but the optical image was used to classify in two classes: simple objects identified by connected pixels and complex objects consisting of separated pixels indicating clustered icebergs. For all six complex objects VV showed higher backscatter than HH, while for all simple objects, except one, HH showed higher backscatter than VV. It is clear that iceberg shape and geometry needs to be better quantified in order to understand the detection capability for the two polarisations. Since future SAR systems will have different polarisation and resolution options, it is important to determine which SAR modes should be used for iceberg detection.

(6) Review of previous airborne surveys and other historical observations was done in order to assess the results of the 2005 and 2006 studies. Direct comparison of statistical iceberg data from previous studies with present satellite studies is not very useful because the observing methods are very different and also the geographical and seasonal coverage of the data. However, all the previous iceberg data are important as background and reference for new data, especially for assessment of the number of icebergs that can occur in different areas at various times of the year. Estimation of probability of iceberg occurrence depends on good archives of data. Iceberg concentration maps, as shown in Fig. 39, documents that the highest density of icebergs are found in the Franz Josef Land archipelago. This agrees with the analysis of the satellite images in chapter 3 and 4. Drift and melting are other important properties of icebergs, but this aspect has not been addressed in the study.

The main conclusions from the study are the following:

(i) Iceberg detection from satellites requires combined use of optical and SAR images of high resolution (≈ 10 m pixels or better). SAR and optical images have complementary properties which are useful for iceberg detection. SAR is good for year round observation and daily observation regardless of cloud cover, but SAR has speckle noise that makes iceberg identification more difficult. Optical images have better detection capability than SAR, but are limited by cloud cover and darkness.

(ii) Icebergs of size 50 m and more can be detected using optical sensors with pixels size of about 15 m (Landsat and ASTER images). By using SAR images with similar pixel size, icebergs less than 50 m are not reliably detected. The speckle noise in SAR images causes many false identifications of icebergs. SAR images also respond to other properties of the icebergs such as shape and geometry, which need to be further studied. By using SAR to detect icebergs more reliably, the image resolution must be increased. With RADARSAT-2 and TerraSAR-X, it will be possible to use SAR data with resolution of 3 – 5 m. In the Barents Sea where most of the icebergs are small (< 100m) detection capability will increase significantly by use of this resolution. However, higher resolution is obtained at the expense of the spatial coverage.

(iii) Iceberg detection depends on the background. The possibility to use optical and SAR images to observe icebergs under different background conditions are the following:
   • Icebergs in fastice near calving areas: optical images produce shadows against the background fastice, which is usually well-defined. Image resolution determines the size of the icebergs to be observed. Stationary ice means that there is good possibility to identify icebergs over longer time periods and that timing of the image acquisition is flexible.
   • Icebergs in open water: icebergs will appear as bright spots against dark background for both optical and SAR images, provided that optical images have minimal cloud cover and that wind speed is low for the SAR images. Higher wind reduces the contrast between open water and icebergs and makes detection more difficult in SAR images.
   • Icebergs in drifting ice: iceberg will create tracks in the drifting ice if there are larger floes of consolidated ice. These tracks are visible both in optical and SAR images. If the surrounding sea ice has variable concentration and floe size, it is difficult to distinguish icebergs from background both for optical and SAR.

(iv) Validation of satellite observations by aircraft and ship data is an essential part of the study, and we were to some extent able to include data from the Somov expeditions both in 2005 and 2006. For this purpose we made efforts to find satellite images that were co-localised with the Somov data. Positions of icebergs from satellite analysis could be compared with position data from ship and helicopter with good results. The number of icebergs obtained from satellite analysis was in some cases much larger than the number provided by the field observations, but we were not able to check these results. For example, our analysis of satellite images showed that about 250 icebergs were found within 10000 km^2 south of Franz Josef Land, while the report by Abramov and Zubakin (1992) showed a maximum iceberg concentration of between 50 and 100 in the same region. It would have been very useful to compare a systematic mapping of icebergs by in situ observations with satellite image analysis, but we were not able to get hold of such data from AARI. Further comparison using data on height, shape and geometry of individual icebergs were not done, but will be particular important for validation of SAR.

(v) Ordering of satellite data for specific areas and days is also essential in order to obtain the relevant data for the study. For 2005 only archived data could be obtained, and the satellite data archives have very limited data for remote areas such the north-eastern Barents Sea. Successful use of satellite data requires careful planning and ordering of data. For the 2006

data, this was done to some extent because we had information about the area where Somov planned to operate. For optical images, we put in a continuous order for Landsat images, which made it possible to look at every quicklook before we decided which images to ordered and analysed. For SAR data we put in orders 2 weeks in advance, but the risk is that the ship can decide to change its sailing plan so that the SAR image is not co-located with the field measurements. The coordination between satellite data ordering and the field operations was only partly successful.

Recommendations:

(A) Explore detection capability with new SAR and high resolution optical images

New SAR satellites which will operate in the next 5 – 10 years such as RADARSAT-2, TerraSAR-X, and Sentinel-1, will have several modes allowing users to select scan width, resolution and polarisation. For iceberg monitoring, we have performed some tests comparing HH- and VV-polarisation. Further studies of cross- (HV, VH) and co-polarization (HH, VV) as well as variable resolution and incidence angle for detection of icebergs should be performed in focused experiments Franz Josef Land and Novaya Zemlya where the size and shape of the icebergs are measured. RADARSAT-2 and TerraSAR-X, which are scheduled for launch in 2007, will provide SAR images with pixel size down to 2 – 3 m and all four polarisations. Before RADARSAT-2 and TerraSAR-X data become available, it will be useful to do further studies of ENVISAT Alternating Polarisation images which are available at low cost. In parallel with use of SAR images, optical images from ASTER, LANDSAT and SPOT should be used to estimate the number of icebergs in various regions and for validation of SAR observations. While Landsat and ASTER can be obtained at relatively low cost, the spatial coverage is rather limited. With SPOT it will be possible to have better spatial as well as temporal coverage, but the cost of data is higher. SPOT can also deliver images at 5 m pixels size in 60 by 60 km. SPOT can provide stereo photographs to study iceberg height and geometry. The results of such focused study will an assessment of the detection capability of the satellite data. This will serve as background for setting up an operational iceberg monitoring scheme where satellite SAR and optical images are the major data sources.

(B) Observation of the seasonal evolution of iceberg distribution

The seasonal and interrannual variability in iceberg populations in the north-eastern Barents Sea should be investigated by combined use of optical and SAR images, as outlined in (A). The seasonal evolution of iceberg populations can be studied by repeating the data coverage once per month from April through September. Ordering of optical images should ensure that data are taken every day, but only good quality image are obtained for analysis. We established such agreement with the SPOT data distributor in 2006. This task should be combined with field experiments with ice-going vessels where ARGOS/GPS drifters are placed on selected icebergs to monitor their drift. Iceberg drift data will be important input to iceberg modelling and forecasting. Furthermore, methods for automated identification of icebergs in satellite images should be investigated. For optical data, the characteristic bright object with dark shadow in the northern side is the criterion that should be implemented in an automated algorithm. For SAR images, an algorithm that can recognise objects that are most likely icebergs should be tested. For this study, it is important that some icebergs are tagged with ARGOS /GPS in order to know that the same icebergs are observed repeatedly over time.

 (C) Coordination of field work with satellite observations

In the previous field experiments, there was no coordination between the satellite data work and the field work performed from ship and helicopter. In the 2006 field work, we received some information about planned working area for the ship, which was very useful for ordering satellite

data. But during the course of the field experiment we got very limited information about the positions and flight tracks of the helicopter. Because we did not have sufficient information about the field activities, many of the satellite images were obtained outside the area of the field work, and we could only perform limited of the satellite observations. In future field experiments it will be essential to have good coordination of satellite data analysis and the field activities. This requires daily exchange of information and data, which should be an easy task if the ship has state-of-art communication equipment. The field work should include systematic surveys of iceberg areas south of Franz Josef land and on the west coast of Novaya Zemlya, using helicopter and/or fixed wing aircraft, flying inside an area covered by satellite images, for example 60 by 60 km for ASTER and SPOT images and 100 by 100 km for SAR alternating polarisation images.

(D) Scenarios for monitoring icebergs using satellites, aircraft and ice buoys.

The strategy for monitoring icebergs should include three scales of observation: (1) regional monitoring of the whole north-eastern Barents Sea; (2) monitoring of the most important calving areas in Franz Josef land, Novaya Zemlya and Nordaustlandet, (3) tactical monitoring of areas around offshore platforms and constructions, in case icebergs drift into these areas.

Scenario 1. Year-round observations
The regional monitoring should be done year-round with combined SAR and optical data, supplemented by aircraft flights, and by deployment of ARGOS/GPS drifters on selected icebergs. Iceberg maps should be produced monthly for the spring-summer, and bimonthly for the rest of the year. In the iceberg producing areas, mapping of iceberg populations should be done weekly or biweekly, for estimation of the number of icebergs leaving the production areas and drift away driven by winds and currents. Tactical monitoring around platforms will require more detailed observations in real-time, using ship radar and helicopter surveillance flights. Icebergs velocity should be measured by ARGOS/GPS buoys and the data should be used in combination with models to predict the iceberg drift.

The regional monitoring scheme should be based on a combination of SAR and optical images, using mainly optical images in the April-September period, and mainly SAR images in the dark season. SAR should also be used in the summer if there are long periods of cloud cover. Production of monthly iceberg charts for the area north of 76 N would require 10 – 15 images per month of type Landsat and SAR wideswath. During one year this will amount to 150 – 200 images. In the coastal regions where icebergs are produced, more frequent observations should be made to estimate the flux of icebergs out of the production areas. About 10 ARGOS/GPS drifter should be deployed on icebergs in March- April in order to follow their drift.

Scenario 2. Seasonal observations
A reduced scheme would be to only monitor icebergs from April to September, assuming that the most important period is the spring and summer. The same method and geographical area as for year-round observations would be used, but the need for satellite data would be reduced.

Scenario 3. Tactical information surrounding platforms and constructions.
 The same satellite data would be used as for scenario 1 and 2. In addition, use of helicopter and aircraft for surveillance flights would be needed. The amount of aircraft data will depend on how much information can be derived from the satellite data. The main information, however, will come form the aircraft surveys. If icebergs are found within 100 – 200 km from a platform, the icebergs would be equipped with ARGOS/GPS buoys to monitor exact position and drift.

Costs of satellite data

There are highly variable costs for the satellite data to be used in iceberg observations. At present the cheapest data are the ASTER images (100 USD per image) and the Landsat image (300 USD per image). ASAR data from ESA are provided at about 1000 USD per image. The most expensive data, and also the best user service, are SPOT and RADARSAT, both providing images at about 3000 USD per image. One scenario is to use 100 Landsat/ASTER, 100 ASAR, 10 SPOT and 10 RADARSAT in one year at a cost of about 200.000 USD. If there is a need to increase the use of SPOT and RADARSAT by for example 50 images, the cost would increase by about 150.000 USD.

The cost of satellite data need to be balanced against the cost of using other observing systems, especially aircraft surveys, ship and helicopter observations and deployment of ARGOS/GPS buoys. An optimal observing system need to combine all these elements.

8. References

Abramov, V. and G. K. Zubakin. Russian iceberg observations 1970-1989, OKN IDAP report, December 1992, 37 pp.

Abramov, V. Atlas of Arctic Icebergs. Backbone Publishing Company, 1996, 70 pp.

Danilov, A. I., G. K. Zubakin, and Yu P. Gudoshnikov. Technical Report on the project "CARRYING-OUT OF MULTIDISCIPLINARY ICE RESEARCH ACTIONS IN THE REGION OF SHTOKMAN GAS-CONDENSATE FIELD (SGCF) IN APRIL, 2005", 287 pp, Arctic and Antarctic Research Institute, St. Petersburg. 2005.

Hønsi, I., 1988, "Isfjell i Barentshavet", Stavanger.

Kloster, K. and W. Spring, Iceberg and glacier mapping using satellite optical imagery during the sea ice data acquisition programme (IDAP). Proceedings of POAC 1993, pp. 413 – 424.

Knapskog, A. O., (1996) Assessment of RADARSAT for detection and classification of icebergs. MSc Thesis (in Norwegian), Norwegian Technical University, Trondheim, Norway, 72 pp.

Kvitrud, A., and Hønsi, I., 1991, "Icebergs in the Norwegian Continental Shelf in 1880-1891", Proceedings OMAE-91, Stavanger.

Sandven, S, K. Kloster and O. M. Johannessen. Remote sensing of icebergs in the Barents Sea during SIZEX89. Presented at First International Offshore and Polar Engineering Conference, Edinburgh, 1991.

Spring, W. Ice Data Acquisition Summary Report, MOBIL Research and Development Corporation, Dallas, Texas, February 1994, 140 pp.

Zubakin, G. K., A. K. Naumov and I. V. Buzin. Estimates of ice and icebergs spreading in the Barents Sea. Paper no. 2004-JSC-381, 8 pp, 2004.